The Astrophysical Journal Supplement Series, 160:401–422, 2005 October

THE ORIGIN OF T TAURI X-RAY EMISSION: NEW INSIGHTS FROM THE *CHANDRA* ORION ULTRADEEP PROJECT

Thomas Preibisch,[1] Yong-Cheol Kim,[2] Fabio Favata,[3] Eric D. Feigelson,[4] Ettore Flaccomio,[5] Konstantin Getman,[4] Giusi Micela,[5] Salvatore Sciortino,[5] Keivan Stassun,[6] Beate Stelzer,[5,7] and Hans Zinnecker[8]

Received 2004 December 22; accepted 2005 June 17

ABSTRACT

The *Chandra* Orion Ultradeep Project (COUP) provides the most comprehensive data set ever acquired on the X-ray emission of pre–main-sequence stars. In this paper, we study the nearly 600 X-ray sources that can be reliably identified with optically well-characterized T Tauri stars (TTSs) in the Orion Nebula Cluster. With a detection limit of $L_{\rm X,\,min} \sim 10^{27.3}$ ergs s^{-1} for lightly absorbed sources, we detect X-ray emission from more than 97% of the optically visible late-type (spectral types F–M) cluster stars. This proves that there is no "X-ray–quiet" population of late-type stars with suppressed magnetic activity. We use this exceptional optical, infrared, and X-ray data set to study the dependencies of the X-ray properties on other stellar parameters. All TTSs with known rotation periods lie in the saturated or supersaturated regime of the relation between activity and Rossby numbers seen for main-sequence (MS) stars, but the TTSs show a much larger scatter in X-ray activity than that seen for the MS stars. Strong near-linear relations between X-ray luminosities, bolometric luminosities, and mass are present. We also find that the fractional X-ray luminosity $L_{\rm X}/L_{\rm bol}$ rises slowly with mass over the 0.1–2 $M_\odot$ range. The plasma temperatures determined from the X-ray spectra of the TTSs are much hotter than in MS stars but seem to follow a general solar-stellar correlation between plasma temperature and activity level. The scatter about the relations between X-ray activity and stellar parameters is larger than the expected effects of X-ray variability, uncertainties in the variables, and unresolved binaries. This large scatter seems to be related to the influence of accretion on the X-ray emission. While the X-ray activity of the nonaccreting TTSs is consistent with that of rapidly rotating MS stars, the accreting stars are less X-ray active (by a factor of ~2–3 on average) and produce much less well-defined correlations than the nonaccretors. We discuss possible reasons for the suppression of X-ray emission by accretion and the implications of our findings on long-standing questions related to the origin of the X-ray emission from young stars, considering in particular the location of the X-ray–emitting structures and inferences for pre–main-sequence magnetic dynamos.

Subject headings: open clusters and associations: individual (Orion Nebula Cluster) — stars: activity — stars: magnetic fields — stars: pre–main-sequence — X-rays: stars

1. INTRODUCTION

1.1. *X-Ray Emission from Young Stellar Objects*

Young stellar objects (YSOs) in all evolutionary stages from Class I protostars to zero-age main-sequence (ZAMS) stars show highly elevated levels of X-ray activity (for recent reviews on the X-ray properties of YSOs and on stellar coronal astronomy in general, see Feigelson & Montmerle 1999 and Favata & Micela 2003). X-ray observations of star-forming regions allow us to study the high-energy processes in YSOs, which are of great importance for our understanding of the star formation process. For example, the X-ray emission from a YSO should photoionize its circumstellar material and thus influence accretion as well as outflow processes, both of which are thought to be based on the interaction of ionized material with magnetic fields. The X-ray emission from the central YSO is certainly an important, probably even the dominant, factor in determining the ionization structure of protoplanetary disks, and it has therefore a strong impact on processes like the formation of protoplanets (e.g., Glassgold et al. 2000; Matsumura & Pudritz 2003).

The first discoveries of X-ray emission from T Tauri stars (TTSs, low-mass pre–main-sequence [PMS] stars) were made with *Einstein* (e.g., Feigelson & DeCampli 1981) and revealed a surprisingly strong X-ray activity, exceeding the solar levels by several orders of magnitude. The X-ray observations also revealed a new population of YSOs (Walter et al. 1988), the "weak-line T Tauri stars" (WTTSs), which lack the classical optical signposts of youth, such as strong Hα emission, of the previously known "classical T Tauri stars" (CTTSs). The *ROSAT* observatory increased the number of observed star-forming regions, and thereby the number of known X-ray–emitting TTSs, considerably (e.g., Feigelson et al. 1993; Casanova et al. 1995; Gagné et al. 1995; Neuhäuser et al. 1995; Preibisch et al. 1996). The *ROSAT* All Sky Survey led to the X-ray detection of extended populations of TTSs in and around many star-forming regions (e.g., Neuhäuser 1997) and demonstrated that the stellar

[1] Max-Planck-Institut für Radioastronomie, Auf dem Hügel 69, D-53121 Bonn, Germany.
[2] Astronomy Department, Yonsei University, Seoul, South Korea.
[3] Astrophysics Division, Research and Science Support Department of ESA, ESTEC, Postbus 299, 2200 AG Noordwijk, Netherlands.
[4] Department of Astronomy and Astrophysics, Pennsylvania State University, University Park, PA 16802.
[5] INAF, Osservatorio Astronomico di Palermo G. S. Vaiana, Piazza del Parlamento 1, I-90134 Palermo, Italy.
[6] Department of Physics and Astronomy, Vanderbilt University, Nashville, TN 37235.
[7] Dipartimento di Scienze Fisiche ed Astronomiche, Università di Palermo, Piazza del Parlamento 1, I-90134 Palermo, Italy.
[8] Astrophysikalisches Institut Potsdam, An der Sternwarte 16, D-14482 Potsdam, Germany.

populations of star-forming regions are considerably larger than those suspected by earlier surveys based on classical youth indicators such as Hα emission. The *ROSAT* All Sky Survey was also well suited to study the X-ray properties in complete, volume-limited samples of nearby field stars. An important result from such studies was that apparently all cool dwarf stars are surrounded by X-ray–emitting coronae, with a minimum X-ray surface flux around 10^4 ergs s^{-1} cm^{-2} Schmitt (1997). The *ASCA* satellite detected X-ray emission from numerous deeply embedded YSOs; due to its rather poor spatial resolution, however, the proper identification of the X-ray sources was often difficult.

While the X-ray missions of the last two decades provided important information about the X-ray properties of YSOs, there were also serious limitations. First, the typical samples of X-ray–detected objects in young clusters and star-forming regions contained hardly more than $\sim$100 objects, too few to allow well-founded statistical conclusions to be drawn. Second, a large fraction of the known cluster members (especially low-mass stars) remained undetected in X-rays, and any correlation studies had therefore to deal with large numbers of upper limits. Third, especially in dense clusters, the individual sources could often not be spatially resolved, and so the proper identification of the X-ray sources was difficult or impossible. Finally, only a relatively small number of individual young stars were bright enough in X-rays to allow their spectral and temporal X-ray properties to be studied in detail, and it is not clear whether these stars really are "typical" cases or perhaps peculiar objects.

With the advent of *Chandra* and *XMM-Newton*, the situation has improved substantially. Due to the large collecting areas of these observatories, their sensitivity is at least an order of magnitude better than that of earlier missions. Due to their wide energy band, extending from $\sim$0.2–0.5 keV up to $\sim$8–10 keV, they are very well suited to study the hard X-ray emission from highly obscured YSOs (e.g., Skinner et al. 2003). Furthermore, *Chandra* has a superb point-spread function, providing a spatial resolution of better than $1''$; this abolishes the usual identification problems in nearby star-forming regions.

1.2. *Open Questions about the X-Ray Activity from TTSs*

We enunciate two basic, still unresolved questions concerning the origin of the elevated X-ray activity of TTSs: Does the strong X-ray activity of TTSs, with X-ray luminosities up to $\sim 10^4$ times higher and plasma temperatures up to $\sim$50 times higher than those seen in our Sun, originate from solar-like coronae? If so, are these coronae created and heated by solar-like (although strongly enhanced) magnetic dynamo processes, or are fundamentally different magnetic structures and heating mechanisms involved?

One main obstacle on the way toward an understanding of TTS X-ray activity is the fact that the solar corona has an extremely complex and dynamic structure with many different facets (e.g., Aschwanden et al. 2001); it is not clear to what degree comparisons and extrapolations from the solar to the stellar case make sense. A second problem is that even for the Sun, which can be studied in great detail at high spatial, temporal, and spectral resolution, the important question about the heating of the solar corona remains puzzling, even after 5 decades of intense research (e.g., Walsh & Ireland 2003). The third problem is our lack of a sound understanding of the dynamo processes, which are the ultimate origin of the magnetic activity in the Sun and in stars (e.g., Ossendrijver 2003).

The X-ray activity of main-sequence (MS) stars is mainly determined by their rotation rate. The well-established rotation-activity relation (e.g., Pallavicini et al. 1981; Pizzolato et al. 2003) is given by the power-law relation $L_X/L_{bol} \propto P_{rot}^{-2.6}$, in agreement with the expectations from solar-like $\alpha - \Omega$ dynamo models (e.g., Maggio et al. 1987). At periods shorter than $\sim$2–3 days, the activity saturates at $\log(L_X/L_{bol}) \sim -3$ for reasons that are not yet understood. The plasma temperatures generally increase with the level of X-ray activity, scaling roughly as $T_X \propto (L_X/L_{bol})^{0.5}$ (e.g., Preibisch 1997). Most TTSs rotate quite rapidly, and neither their X-ray luminosities nor their plasma temperatures are unusual when compared to rapidly rotating MS stars.

However, a relation between rotation and X-ray activity could never be convincingly established for TTSs; in most studies the small number of X-ray–detected TTSs with known rotation periods did not allow us to draw sound conclusions. This problem of small and often biased samples has, however, recently been overcome with two *Chandra* studies of the Orion Nebula Cluster (ONC) (Feigelson et al. 2002a; Flaccomio et al. 2003b), both of which found *no significant relation between X-ray activity and rotation*. This strongly puts into question the solar-like dynamo activity scenario for TTSs. Another argument against solar-like dynamos comes from theoretical considerations: at ages of only a few Myr, the TTSs are usually thought to be fully convective, and therefore the standard solar-like α-Ω dynamo, which is anchored at the boundary between the convective envelope and the inner radiative core, should not work. Theoreticians have developed alternative dynamo concepts (e.g., Küker & Rüdiger 1999; Giampapa et al. 1996) that may work in fully convective stars. A problem with these and other models is that they usually do not make quantitative predictions that can be easily tested from observations. Further possibilities for the origin of X-ray emission from TTSs include magnetic fields coupling the stars to their surrounding circumstellar disk (see, e.g., Hayashi et al. 1996; Montmerle et al. 2000; Isobe et al. 2003; Romanova et al. 2004) or X-ray emission from accretion shocks (see, e.g., Kastner et al. 2002; Stelzer & Schmitt 2004; Favata et al. 2003, 2005). The investigation of these possibilities in the light of the *Chandra* Orion Ultradeep Project (COUP)[9] data will be a major topic of this study.

1.3. *Properties of the ONC and Previous X-Ray Observations*

The Orion Nebula is an H II region on the near side of a giant molecular cloud, which contains one of the most prominent and nearby ($D \sim 450$ pc) star-forming regions (for a recent review, see O'Dell 2001). This star-forming region contains a massive cluster of young ($\approx 10^6$ yr) stars (cf. Herbig & Terndrup 1986; McCaughrean & Stauffer 1994; Hillenbrand 1997), which is known as the Orion Nebula Cluster (ONC). The Orion Nebula is illuminated mainly by the two O-type stars θ^1 Ori C and θ^2 Ori A. Since the ONC is a perfect laboratory for observations of star formation over the full stellar mass range, it is one of the best investigated star-forming regions and has been observed at virtually every wavelength. Hillenbrand (1997) has compiled a catalog of nearly 1600 optically visible stars within $\sim$2.5 pc of the Trapezium; for over 900 of these stars enough information is available to place them into the H-R diagram and to determine their masses and ages by comparison with theoretical PMS evolution models.

The ONC has been observed with basically all previous X-ray observatories (see, e.g., Ku & Chanan 1979 for *Einstein* observations; Gagné et al. 1995, Geier et al. 1995, and Alcalá et al. 1996 for *ROSAT* observations; and Yamauchi et al. 1996 for *ASCA*

[9] Links to the COUP data set are available in the electronic edition of the *Supplement*.

observations). However, the high spatial density of stars in the ONC and the poor spatial resolution of these X-ray observatories did not allow a reliable identification of many X-ray sources. Only *Chandra* with its superb point-spread function is suitable for studying the ONC, where the mean separation between the sources in the inner $1'$ radius area is only $5''$. The ONC has been observed with both imaging instruments on board *Chandra*. The results of two Advanced CCD Imaging Spectrometer observations with a combined exposure time of 23 hr were reported in Garmire et al. (2000) and Feigelson et al. (2002a, 2002b, 2003). A total of 1075 individual sources were detected, 91% of which could be identified with known stellar members of the cluster. Flaccomio et al. (2003a, 2003b) presented the analysis of a 17.5 hr High Resolution Camera (HRC) observation of the ONC, which yielded 742 X-ray sources in the $30' \times 30'$ field of view. Furthermore, some of the brightest X-ray sources in the ONC have also been studied with the High Energy Transmission Grating Spectrometer (Schulz et al. 2000, 2001, 2003), but most of these sources are massive stars, which are not the topic of this paper.

In this paper, we discuss the X-ray data on the TTSs in the ONC resulting from COUP, by far the longest and most sensitive X-ray observation ever obtained for the ONC. The plan of this paper is as follows: after briefly describing the COUP observation in § 2, we define in § 3 the optical sample that will be the basis of our studies and then investigate the relation of the X-ray emission to basic stellar parameters in § 4. In § 5 we study in detail the relation between X-ray emission, rotation and convection. In § 6 we discuss the origin of the large scatter seen in the correlations between X-ray activity and other stellar parameters. In § 7, we investigate the plasma temperatures as determined from the fits to the X-ray spectra. Section 8 deals with the possible connections between X-ray emission and circumstellar accretion disks. Finally, in § 9 we discuss the implications of our results with respect to the origin of the TTS X-ray emission.

2. THE COUP OBSERVATION

The COUP observation is the deepest and longest X-ray observation ever made of a young stellar cluster, providing a rich and unique data set for a wide range of science studies. The observational details and a complete description of the data analysis can be found in Getman et al. (2005a), here we summarize only the aspects that are most important to our studies. The COUP observation was performed between 2003 January 8 and 21, utilizing the Advanced CCD Imaging Spectrometer (ACIS) in its imaging configuration, which gives a field of view of $17' \times 17'$. The total exposure time of the COUP image was 838,100 s (232.8 hr or 9.7 days). The spatial resolution of ACIS is better than $1''$ over most of the field of view. The very low background allows the reliable detection of sources with as little as $\sim$5 source counts. The final COUP source catalog lists 1616 individual sources. The superb point-spread function and the high accuracy of the aspect solution allowed a clear and unambiguous identification of nearly all X-ray sources with optical or near-infrared counterparts.[10]

Spectral analysis was performed using a semiautomated approach to produce an acceptable spectral model for as many as possible sources. The XSPEC spectral fitting program was used to fit the extracted spectra with one- or two-temperature optically thin thermal plasma MEKAL models assuming 0.3 times solar abundances and X-ray absorption. The parameters derived in these fits are the hydrogen column density $N_{\rm H}$ as a measure of the X-ray absorption and the temperatures $T_{\rm X}$ and emission measures of the one or two spectral components. The spectral fitting results were also used to compute the intrinsic (extinction-corrected) X-ray luminosity by integrating the model source flux over the 0.5–8 keV band.

Our analysis in this paper is based on the tabulated X-ray properties and identifications of the COUP sources as listed in Getman et al. (2005a). We use the identifications of the X-ray sources with optical counterparts as given in their Table 9, the X-ray luminosities and X-ray spectral properties as listed in their Tables 8 and 6, and upper limits of undetected stars in the Hillenbrand sample as given in their Table 11.

The temporal behavior of COUP sources is often very complex, with high-amplitude, rapidly changing flares superposed on apparent quiescent or slowly variable emission as studied in detail by Wolk et al. (2005), Favata et al. (2005), and Flaccomio et al. (2005). For the purpose of the present study, the individual features of the light curves are not of interest. We note that the X-ray properties tabulated in the COUP tables, i.e., the count rates, derived spectral parameters, and X-ray luminosities, represent the average over the 10 days exposure time of our data set. This implies that the effect of short excursions in the X-ray light curves, like flares with typical timescales of a few hours, are strongly "smoothed out." Since most of the young stars are rather fast rotators with periods of less than 10 days, the tabulated X-ray properties represent for these objects the average over at least one rotation period and therefore also smooth out possible rotational modulation.

Nevertheless, it would be interesting to establish the level of "quiescent" X-ray emission in the sources, i.e., the sustained, or "typical" level of X-ray emission outside the periods of flares or otherwise elevated activity. For this purpose, we used the results of the maximum-likelihood blocks (MLBs) light curve analysis (Flaccomio et al. 2005), which segments the light curves into contiguous sequences of constant count rates and allows to discern between periods of flaring and more constant, sustained X-ray emission. A strict and fully convincing definition for "quiescent" X-ray emission is not possible, especially since any apparently quiescent emission may, in reality, just be a superposition of numerous unresolved small flares. Wolk et al. (2005) empirically establish a proxy for the quiescent emission levels by determining a "characteristic level" in each light curve, which is essentially defined as the average count rate over periods where the count rate is not significantly elevated. An estimate for the characteristic X-ray luminosity can then be obtained by multiplying the temporally averaged X-ray luminosity, as determined from the spectral analysis, with the ratio of the characteristic count rate from the MLB analysis to the mean count rate over the COUP exposure. We note that this simple scaling procedure is not fully self-consistent, because it does not take into account that the X-ray spectral parameters (and thereby the transformation factor from count rate to luminosity) can change as a function of the emission level, but it should be appropriate for our purposes.

The difference between the average and characteristic X-ray luminosities is generally not large: the median value of the correction factor is 0.78; for only 13% of the TTSs this factor is $<1/2$, and for only 4% of the TTSs it is $<1/3$. We will show below that the choice of either the average or the characteristic X-ray luminosities has generally very little effect on the observed relations. We will therefore mainly use the temporally averaged X-ray luminosities and consider the characteristic luminosities only in a few cases.

[10] The median offsets between COUP sources and near-infrared or optical counterparts are only $0''.15$ and $0''.24$, respectively.

3. DEFINITION OF THE OPTICAL SAMPLE AND X-RAY DETECTION COMPLETENESS

3.1. *The Optical Sample of ONC Stars*

The aim of our study is to investigate the X-ray properties of a homogenous and well-defined sample of comprehensively characterized TTSs (=young late-type [F–M] stars). We will therefore *not* consider the COUP-detected brown dwarfs (see Preibisch et al. 2005) or embedded objects (see Grosso et al. 2005) or OBA stars (see Stelzer et al. 2005), although we will sometimes compare the more massive stars with TTSs.

The basis for the construction of our "optical sample" is the Hillenbrand (1997, hereafter H97) sample of 1576 optically visible ($I \lesssim 17.5$) stars within $\sim$2.5 pc ($\sim 20'$) of the Trapezium, for the 934 stars whose optical spectral types are known. We used an updated version of the H97 tables in which spectral types and other stellar parameters have been revised for many objects.[11] Some of the stars in this area are unrelated field stars lying either in the foreground or the background of the Orion Nebula; these should of course be excluded from our studies. We therefore used the membership information from proper-motion studies listed in the table of H97: we consider all stars with membership probabilities $\geq$50% to be bona fide members of the ONC, while stars with membership probabilities $<$50% are considered here to be nonmembers and excluded from our analysis. Stars with no membership information are considered here as likely cluster members, because contamination by foreground field stars is very small,[12] and contamination by background stars is unlikely due to the large visual extinction in the molecular cloud immediately behind the ONC. H97 assumes that the optical database is *representative of all stars in the ONC region* and that the completeness of $\sim$60% is uniform with radius.

A total of 1056 of the H97 stars are within the field of view of the COUP observation, 892 of which are detected as X-ray sources. Excluding the 33 stars that are identified as nonmembers, we have 1023 likely ONC members from the H97 sample in the COUP field of view and detect 870 of these (i.e., 85%) as X-ray sources. For the analysis in this paper we use those of these stars for which spectral types are known. Our "optical sample" then consists of 639 optically visible likely ONC members from H97 with known spectral type; 598 of these stars (i.e., 94%) are detected as X-ray sources, while 41 remain undetected in the COUP image. The spectral types range from O7 for θ^1 C Ori, the most massive and luminous star in the ONC, down to $\sim$M6.5 for objects close to the stellar-substellar boundary (at $\sim 0.075\ M_\odot$) at the age of the ONC. For 575 stars in the COUP optical sample bolometric luminosities are known, allowing them to be placed into the H-R diagram. Masses and ages were estimated for 536 stars by comparison of their location in the H-R diagram to the theoretical PMS evolutionary tracks from Siess et al. (2000). The masses in the COUP optical sample range from 0.1 $M_\odot$ (the lowest mass in the Siess et al. 2000 models) to 38 $M_\odot$ for θ^1 C Ori.

The visual extinction is known for 631 of the 639 stars in our optical sample and varies from 0 to $A_V = 11$ mag, with a mean value of $\langle A_V \rangle = 1.55$ mag. Since the optical sample is magnitude limited, extinction introduces a bias, since intrinsically brighter stars can suffer from more extinction and still be included in the sample than the intrinsically fainter stars. We therefore used an extinction limit to construct a more homogeneous sample: we define as the "lightly absorbed optical sample" those stars for which the optical extinction is known and is $A_V \leq 5$ mag. The lightly absorbed optical sample consists of 586 stars, 554 of which are detected as X-ray sources in the COUP image. This extinction limit also yields a rather uniform sample with respect to the X-ray detection limit: PIMMS simulations for Raymond-Smith spectra with $kT = 2$ keV show that the detection limit (i.e., the X-ray luminosity that corresponds to a given number of detected source counts) increases by 0.39 dex when going from zero extinction to $N_{\rm H} = 8 \times 10^{21}$ cm^{-2} ($A_V = 5$ mag). Since the uncertainty of the X-ray luminosity determinations is similar to this factor, our extinction-limited sample does not suffer from a significant extinction-dependent X-ray detection bias.

To summarize, our "lightly absorbed optical sample" of 586 stars is not 100% complete (because spectral types are not available for all stars in the ONC) but nevertheless should be a *statistically representative sample of the ONC young stellar population with low extinction*. The only potential systematic selection effect might be that older ($\gtrsim$10 Myr) very low mass ($M \lesssim 0.2\ M_\odot$) stars may be missing; it is, however, unclear whether such an older population of ONC members does exist at all.

For the 41 stars in the optical sample that were not detected as X-ray sources in the COUP data, we estimated upper limits to their X-ray luminosities from the tabulated upper limits to their count rates following the procedure outlined in Getman et al. (2005a).

3.2. *X-Ray Detection Completeness*

Table 1 lists the COUP X-ray detection fractions for the different spectral types. It is important to note here that most of the nondetections of ONC stars are due to X-ray source confusion in the COUP data; the typical cases are close ($\sim 1''$–$2''$ separation) binary systems, in which only one of the components is clearly detected as an X-ray source (Getman et al. 2005a). In these cases the object would perhaps have been detected if located at a different position. Since the occurrence of source confusion should not depend on stellar parameters, these objects can be considered as "unobserved" and will be ignored in our analysis. We can thus compute an "effective," confusion-free detection fraction by removing these nondetections with source confusion from the sample. Then the effective detection fractions range between 97% and 100% for all spectral classes except the A- and B-type stars. This means that less than 3% of the TTSs in the optical sample are undetected because their X-ray emission is below our detection limit (Fig. 1).

With so few undetected objects, we can look at these stars in detail. The undetected B8 star H97 1892 and the A1 star H97 531 are intermediate-mass stars and will be discussed in Stelzer et al. (2005).

The three undetected K-type stars not suffering from source confusion are H97 62, H97 489, and H97 9320. H97 62 has a rather large extinction of $A_V = 5.26$ mag that may have absorbed too much of its X-ray emission. H97 489 has no bolometric luminosity or optical extinction listed in H97. The third object is the K6-star H97 9320, which lies far (2.7 mag) below the ZAMS in the H-R diagram, putting considerable doubt on its membership to the ONC; since the star has also no proper-motion membership information in H97, we suspect it to be a nonmember and exclude it from our optical sample. We therefore conclude that *all K-type stars in the lightly absorbed optical sample are detected*.

For the 13 undetected M-type stars not suffering from source confusion, we note that two objects have optical extinction

[11] See http://www.astro.caltech.edu/~lah/papers/orion_main.table1.working.

[12] H97 estimates that $\sim$97% of the $I \lesssim 17$ mag stars within about 1 pc of the Trapezium (i.e., roughly the field of view of our COUP image) are ONC members.

TABLE 1
DETECTION FRACTIONS OF ONC STARS IN THE OPTICAL SAMPLE

PROPERTY	SPECTRAL TYPE							
	O	B	A	F	G	K	M0–M6.5	All
Optical Sample								
Detections	2	11	3	1	8	133	441	598
Nondetections	0	1	3	0	0	8	29	41
$\mathcal{F}$ (%)	100	91.7	50.0	100	100.0	94.3	93.6	...
Confusion	0	0	2	0	0	6	17	24
$\mathcal{F}'$ (%)	100	91.7	75	100	100	98.5	97.3	...
Lightly Absorbed Optical Sample								
Detections	2	11	2	1	7	117	414	554
Nondetections	0	1	3	0	0	3	26	32
$\mathcal{F}$ (%)	100	91.7	40.0	100	100	97.5	94.1	94.5
Confusion	0	0	2	0	0	3	15	19
$\mathcal{F}'$ (%)	100	91.7	66.7	100	100	100	97.4	97.7

NOTES.—The quantity $\mathcal{F}$ is the detection fraction; $\mathcal{F}'$ is the detection fraction if objects with nondetections due to X-ray confusion are removed from the sample, which gives the fraction of objects that are below the X-ray detection limit. The COUP undetected K6 star H97 9320, which lies far (2.7 mag) below the ZAMS in the H-R diagram, has been removed from the optical sample.

exceeding $A_V = 5$ mag and four objects have no proper-motion membership information in H97 and may therefore perhaps be nonmembers. Only eight of the M-type stars among the known proper-motion members in the lightly absorbed optical sample remain undetected. The upper limits to the fractional X-ray luminosities of the undetected M-type stars range from $\log(L_X/L_{bol}) < -5.46$ (for H97 305) to $\log(L_X/L_{bol}) < -4.37$ (for H97 853). This is considerably below the mean fractional X-ray luminosities of the detected M-type stars of $\log(L_X/L_{bol}) = -3.62$, but still within the range of fractional X-ray luminosities found for the detected M-type stars, three of which have values below the lowest upper limit for the nondetections. We conclude that the very few undetected M-type stars show low, but not necessarily unusually low, levels of X-ray activity.

To summarize, we find that COUP detects every optically visible star in the ONC sample except a few of the intermediate-mass stars (which are not expected to be intrinsic X-ray emitters) and a few of the M-type stars (some of which may perhaps be nonmembers). *We find no indications for the existence of an "X-ray–quiet" population of stars with suppressed magnetic activity.* Our analysis is thus based on a (nearly) complete sample, and we can be very confident that our conclusions will not be affected by nondetections. The only remaining concern is about the completeness of the optical sample, which may not be very well established for older ($\gtrsim 10^7$ yr) very low mass ($\lesssim 0.2\ M_\odot$) stars.

It is interesting to note that most (1047 of 1616, i.e., 65%) of the COUP X-ray sources were already detected in the previous 23 hr exposure ACIS observation or the 17.5 hr HRC observation of the ONC. Since the field of view covered by the different observations is not identical, we focus on the inner 8′ radius area, which is included in all *Chandra* observations considered here. In this area, 970 (66.6%) of the 1457 COUP sources, 475 (90.9%) of the 522 COUP sources in the optical sample, and 438 (91.3%) of the 480 COUP sources in the lightly absorbed optical sample were already detected in the previous 23 hr ACIS observation or the 17.5 hr HRC observation. With more than 10 times the earlier exposure times, COUP leads to the detection of only a relatively small number of 47 (42) new X-ray sources that could be identified with stars in the (lightly absorbed) optical sample. The COUP data nevertheless represent an important step forward over the previous observations, since they increased the X-ray detection fraction in the lightly absorbed optical sample from ~88% to at least 97%, transforming an incomplete sample to a (nearly) complete sample. Also, the COUP data for the individual sources have much higher signal-to-noise (counts per source) than previous data sets, thus allowing a much more reliable determination of the X-ray source properties.

4. RELATION OF THE X-RAY EMISSION TO BASIC STELLAR PARAMETERS

Since the origin of the X-ray activity in TTSs is still not well known, it is unclear which are the best parameters to consider in making correlations. We therefore consider several possibly useful stellar parameters (bolometric luminosity, stellar mass, effective temperature, rotation, circumstellar disk properties, accretion rates) to look for relations to the X-ray emission level; note that relations between X-ray activity and age are discussed in a separate paper (Preibisch & Feigelson 2005). For the characterization of the X-ray properties we consider here the X-ray luminosity L_X, the fractional X-ray luminosity L_X/L_{bol}, and the X-ray surface flux F_X, i.e., X-ray luminosity divided by the stellar surface area. Throughout this paper, we use L_X to refer to the extinction-corrected total band (0.5–8 keV) luminosity $L_{t,c}$ defined and listed by Getman et al. (2005a).

Most of the relations presented here were already studied in other X-ray data sets (e.g., Feigelson et al. 2003; Flaccomio et al. 2003b; Preibisch & Zinnecker 2002), often with similar results to what we find here. Nevertheless, we study these relations here in some detail because our COUP data provide a unique—in fact the best—data set for an investigation of the nature and the origin of the X-ray emission from TTSs for the following reasons. With the *exceptionally well-characterized young stellar population* in the ONC we can take advantage of known stellar parameters for several hundred stars. The *high sensitivity of the COUP X-ray data* yields a detection limit of $L_{X,\,min} \sim 10^{27.3}$ ergs s^{-1} for lightly absorbed stars and allows us to detect more than 97% of the stars in the lightly absorbed optical sample of cluster members. Our analysis is therefore based on an *nearly complete sample*. The high

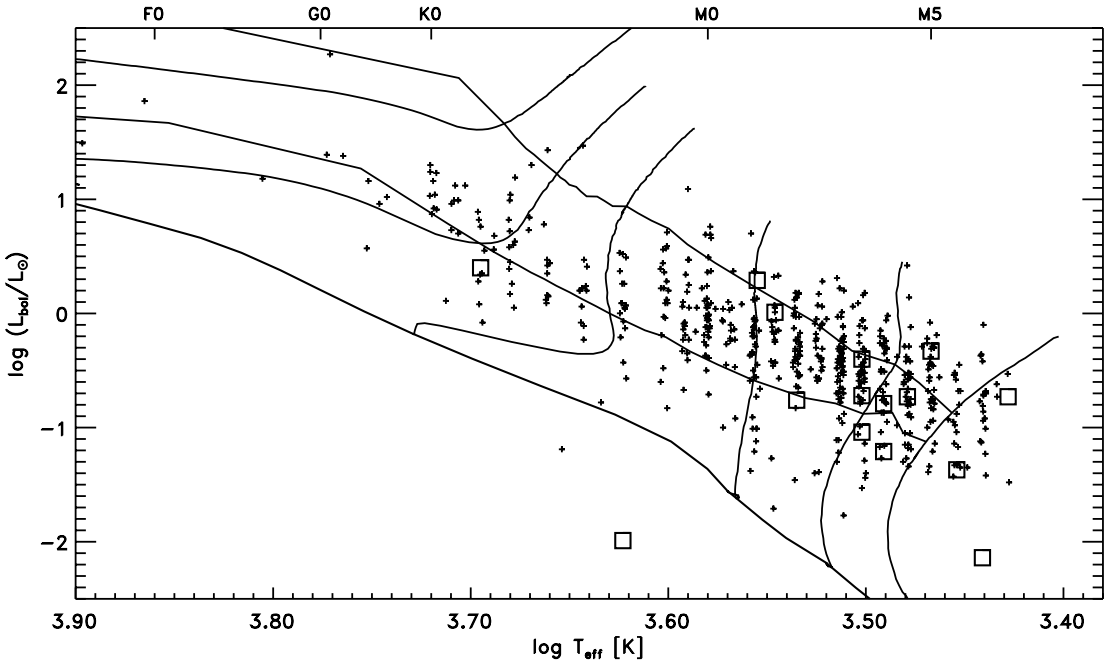

FIG. 1.—H-R diagram for the late-type stars in the optical sample. X-ray–detected objects are plotted as crosses. To avoid the strong overlap of objects with the same spectral types, the log $T_{\rm eff}$-values have been shifted by random numbers in the range $[-0.002,\ +0.002]$. Members of the optical sample that are not detected as X-ray sources and not affected by X-ray source confusion are marked by open squares. The lines show isochrones for ages of 3×10^5 and 3×10^6 yr and the ZAMS and PMS tracks for stellar masses of 0.1, 0.2, 0.4, 1, 2, and 4 $M_\odot$ according to the evolutionary models of Siess et al. (2000). Note that the X-ray–undetected late K-type star well below the ZAMS is very likely not a member of the ONC.

sensitivity allows us to detect X-ray emission of the young solar-luminosity stars down to activity levels[13] of $\log(L_{\rm X}/L_{\rm bol}) \leq -6$. Our statistical analysis strongly benefits from the *large sample* of 598 optically well-characterized ONC stars for which X-ray emission is detected. This represents the largest homogenous sample of TTSs that has ever been studied with very sensitive X-ray observations (and will remain so for the foreseeable future). The *availability of X-ray spectra* with good signal-to-noise for nearly all sources allows the determination of reliable X-ray luminosities. The *10 day long observation* provides a much better measure for the "typical" X-ray properties of the strongly variable TTSs than observations with shorter exposure times, which yield only a "snapshot."

4.1. *X-Ray Luminosity and Bolometric Luminosity*

The plot of X-ray luminosity versus bolometric luminosity is shown in Figure 2. Nearly all stars show $\log(L_{\rm X}/L_{\rm bol}) > -5$ and therefore are much more X-ray active than the Sun [for which $\log(L_{\rm X}/L_{\rm bol}) \sim -6.5$ is an average during the course of the solar cycle]. The most active stars show fractional X-ray luminosities around $\log(L_{\rm X}/L_{\rm bol}) = -3$, which is known as the "saturation limit" for coronally active stars (Fleming et al. 1995).

Considering only the low-luminosity ($L_{\rm bol} < 10\ L_\odot$) stars, we find a clear correlation between X-ray and bolometric luminosity, although with a very large scatter. We utilized the ASURV survival analysis package (Feigelson & Nelson 1985; Isobe et al. 1986; La Valley et al. 1990) for the statistical investigation of the relation between $L_{\rm X}$ and $L_{\rm bol}$. The ASURV software allows one to deal with data sets that contain nondetections (upper limits) as well as detections, and it provides the maximum-likelihood estimator of the censored distribution, several two-sample tests, correlation tests, and linear regressions. The linear regression fit with the parametric estimation maximization (EM) algorithm in ASURV yields $\log(L_{\rm X}[\text{ergs s}^{-1}]) = 30.00(\pm0.04) + 1.04(\pm0.06)\log(L_{\rm bol}/L_\odot)$ with a standard deviation of 0.70 dex in $\log L_{\rm X}$ for the low-luminosity stars ($L_{\rm bol} \leq 10\ L_\odot$). This relation is very similar to the relations found for other young clusters (cf. Feigelson & Montmerle 1999) and is consistent with a linear relation between X-ray and bolometric luminosity characterized by $\langle\log(L_{\rm X}/L_{\rm bol})\rangle = -3.6 \pm 0.7$.

4.2. *X-Ray Activity and Stellar Mass*

Next we considered the relation between X-ray luminosity and stellar mass (Fig. 3). As described in Getman et al. (2005a), the stellar masses listed in the COUP tables were derived from the Siess et al. (2000, hereafter SDF) PMS models. It is well known that mass estimates from PMS evolutionary models are subject to significant uncertainties; different PMS models and/or temperature scales can lead to differences by as much as a factor of $\sim$2 in the mass estimates (for detailed investigations of these uncertainties see, e.g., Luhman 1999 or Hillenbrand & White 2004). As a test to what extent the $L_{\rm X} \leftrightarrow M$ relation is dependent on the choice of the PMS model,[14] we compared the relation found for the masses derived from the SDF models to those based on stellar masses estimated from the PMS models of Palla & Stahler (1999, hereafter PS). Note that the masses determined from these two sets of models agree very well with each other

[13] Note that the quoted activity level refers to the relatively hard 0.5–8 keV COUP band. This band covers most of the X-ray flux from TTSs (which are characterized by rather high plasma temperatures of $\gtrsim$10 MK and have accordingly relatively hard X-ray spectra). Solar-like field stars and the Sun, however, exhibit considerably lower plasma temperatures ($\sim$2 MK in the case of the Sun) and have accordingly softer X-ray spectra, with most of the X-ray flux below the COUP band. If the Sun were located at the distance of the ONC, it would be only marginally detectable during its maximum phase of coronal activity.

[14] Our comparison here is restricted to the PMS models of Siess et al. (2000) and Palla & Stahler (1999) because these two models cover particularly wide ranges of stellar masses; this does not imply that we consider these specific models to be "better" than other models.

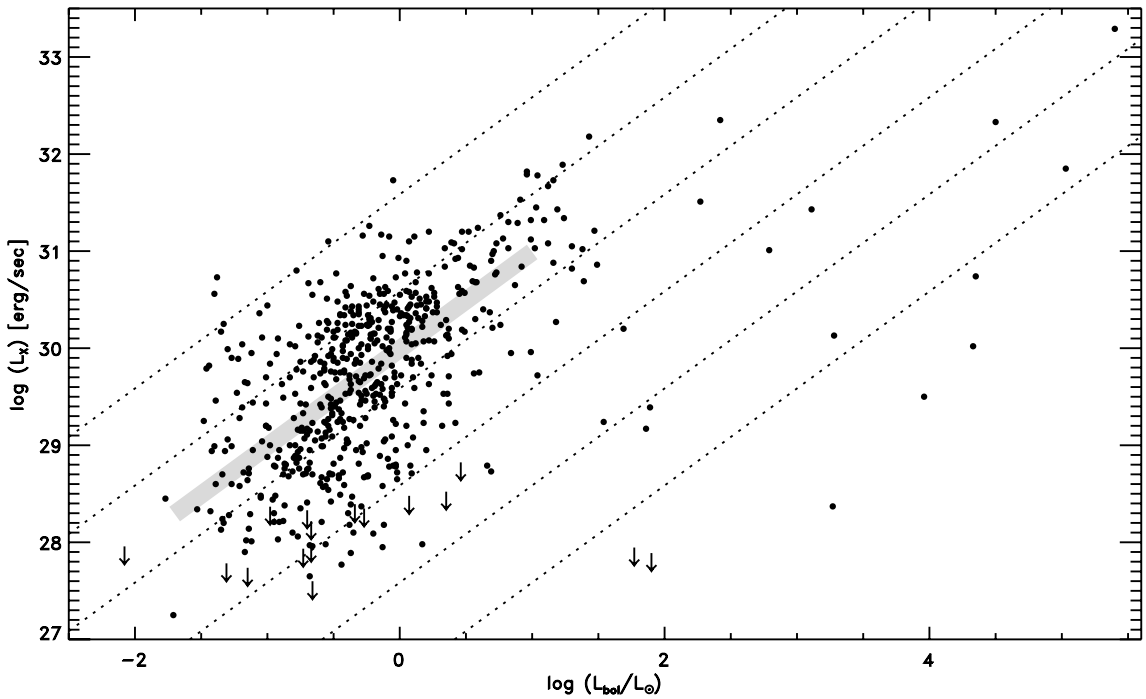

FIG. 2.—X-ray luminosity vs. bolometric luminosity for the stars in the optical sample. For the members of the optical sample that are not detected as X-ray sources in the COUP data, the arrows show the upper limits to their X-ray luminosities. The dotted lines mark $\log(L_X/L_{bol})$ ratios of −2, −3, −4, −5, −6, and −7. The thick gray line shows the EM algorithm linear regression fit for the $L_X \leftrightarrow L_{bol}$ relation for $L_{bol} \leq 10\ L_\odot$ stars computed with ASURV.

for objects with $M > 0.4\ M_\odot$, but below $0.4\ M_\odot$ the PS models yield systematically lower masses than the SDF models.

For both sets of stellar masses a clear correlation is found between X-ray luminosity and mass. For the low-mass ($M \leq 2\ M_\odot$) stars, the SDF models lead to an EM linear regression fit of $\log(L_X[\text{ergs s}^{-1}]) = 30.37(\pm0.06) + 1.44(\pm0.10)\log(M/M_\odot)$ with a standard deviation of 0.65, whereas the PS models yield a somewhat shallower relation of $\log(L_X\ [\text{ergs s}^{-1}]) = 30.34(\pm0.05) + 1.13(\pm0.08)\log(M/M_\odot)$ with a standard deviation of 0.64. From this exercise we conclude that the detailed shape of the $L_X \leftrightarrow M$ correlation does depend on the PMS model used, but the general dependence is independent of the choice of the model.

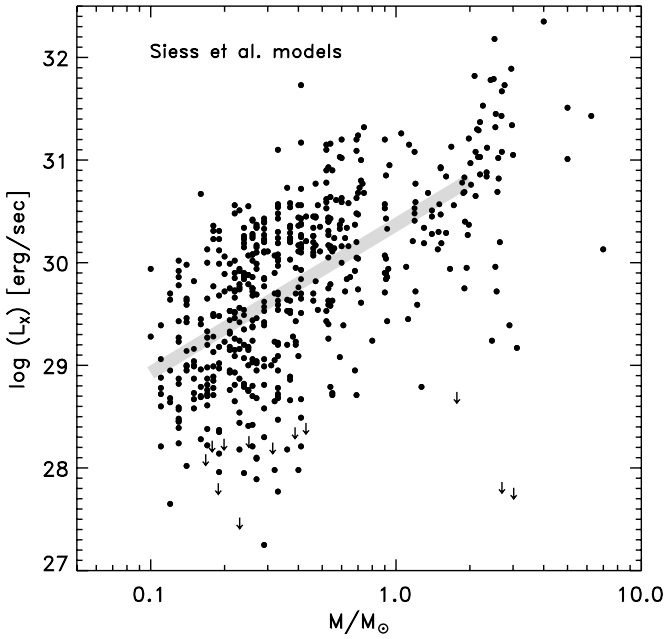

FIG. 3.—X-ray luminosity vs. stellar mass for the stars in the optical sample based on masses determined with the PMS models of Siess et al. (2000). The thick gray line shows the linear regression fit to the low-mass ($M \leq 2\ M_\odot$) stars with the EM algorithm computed with ASURV.

The power-law slopes we find here for the ONC TTSs are considerably lower than those found for the TTSs in the Chamaeleon star-forming region (slope = 3.6 ± 0.6 in the mass range 0.6–2 $M_\odot$; Feigelson et al. 1993) and the very young stellar cluster IC 348 (slope = 2.0 ± 0.2 in the mass range 0.1–2 $M_\odot$; Preibisch & Zinnecker 2002) or than that derived for M-type field stars (slope = 2.5 ± 0.5 in the mass range 0.15–0.6 $M_\odot$; Fleming et al. 1988). The differences in the slopes are in part due to differences in the considered mass ranges and in the methods used to estimate stellar masses. Another factor may be that many of the previous studies had to deal with large numbers of X-ray upper limits for undetected very low mass stars, which perhaps caused the typical X-ray luminosities of these very low mass stars to be underestimated.

Next we consider the fractional X-ray luminosity as a function of mass. In Figure 4 we show the $L_X/L_{bol} \leftrightarrow M$ relation for low-mass stars. The statistical tests in ASURV reveal a very shallow but nevertheless highly significant [$P(0) < 10^{-4}$] correlation between fractional X-ray luminosity and mass for low-mass ($M < 2\ M_\odot$) objects. The linear regression fit with the EM algorithm yields $\log(L_X/L_{bol}) = -3.40(\pm0.06) + 0.42(\pm0.11)\log(M/M_\odot)$ with a standard deviation of 0.69 dex.

We also used this relation to illustrate the influence of X-ray variability during the COUP observation on the resulting correlations. If we consider the *characteristic* X-ray luminosities derived from the MLB light curve analysis rather than the *average* X-ray luminosities, we find a very similar relation with $\log(L_{X,\,char}/L_{bol}) = -3.56(\pm0.05) + 0.40(\pm0.10)\log(M/M_\odot)$ with a standard deviation of 0.64 dex. This test shows that the

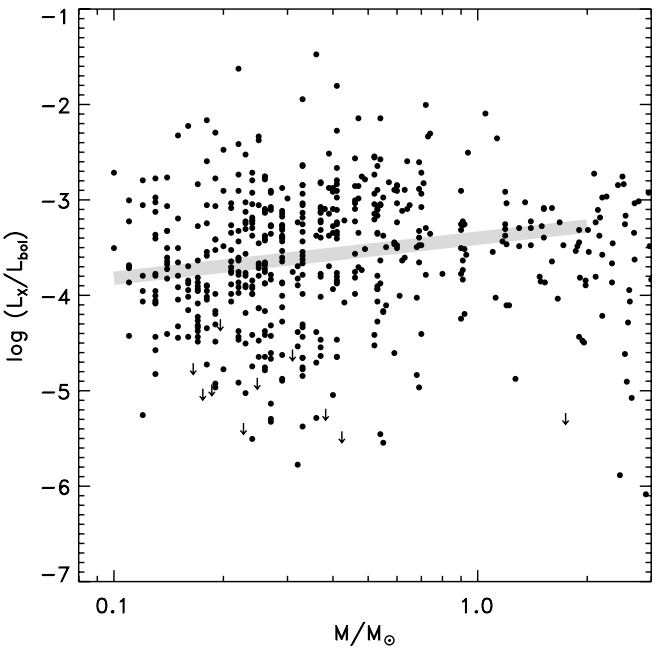

FIG. 4.—Fractional X-ray luminosity vs. stellar mass for the low-mass stars in the COUP optical sample. The line shows the linear regression fit for the low-mass stars ($M \leq 2\ M_{\odot}$) with the EM algorithm computed with ASURV.

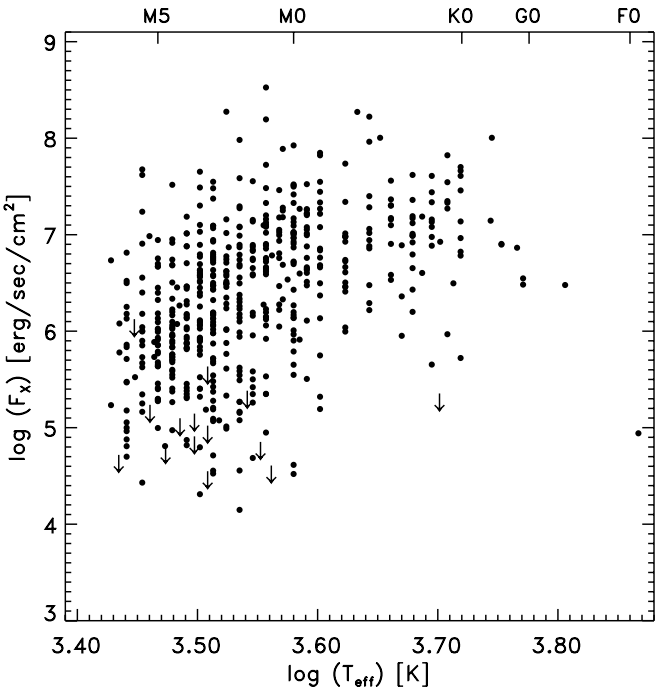

FIG. 5.—X-ray surface flux vs. effective temperature for the TTSs in the optical sample.

use of the characteristic rather than the average X-ray luminosities decreases the values of the fractional X-ray luminosities slightly, but the power-law slopes for the $L_X/L_{bol} \leftrightarrow M$ correlations are nearly identical, and the scatter in the correlation diagrams is only very slightly smaller. From this exercise, we conclude that the correlations do not significantly depend on the choice of the average or characteristic X-ray luminosities.

4.3. *X-Ray Activity and Stellar Effective Temperature*

In Figure 5 we show the X-ray surface fluxes (i.e., X-ray luminosities divided by the stellar surface area) of the ONC TTSs plotted versus their effective temperatures. Nearly all stars have X-ray surface fluxes in the range 10^4–10^8 ergs cm^{-2} s^{-1}, which corresponds nicely to the minimum and maximum X-ray surface flux found for different structures in the solar corona (where coronal holes and the background corona show X-ray fluxes around 10^4 ergs cm^{-2} s^{-1}, while active regions show fluxes up to 10^8 ergs cm^{-2} s^{-1}); the similarity of the X-ray surface flux ranges found for late-type stars and for different constituents of the solar corona has already been noted, e.g., in Schmitt (1997) and Peres et al. (2004). The plot also shows a strong decline of the X-ray surface flux with effective temperature among the M-type stars. This dependence is much more pronounced than the very shallow relation between L_X/L_{bol} and the stellar mass discussed above. This effect can be understood if one recalls that the surface flux and the fractional X-ray luminosity are related to each other by $F_X \propto T_{eff}^4 (L_X/L_{bol})$. Therefore, F_X decreases with decreasing T_{eff} for constant L_X/L_{bol}.

4.4. *Comparison to Main-Sequence Stars*

For a meaningful comparison of the ONC TTSs to MS stars, it is important to keep in mind that our ONC TTS sample is an *optically selected and representative sample* of cluster members. For a proper comparison we therefore have to use an optically selected (not X-ray–selected) sample of MS stars. A well-suited comparison sample is the NEXXUS database (Schmitt & Liefke 2004), which provides updated *ROSAT* X-ray and optical data (including accurate *Hipparcos* parallaxes) for nearby field stars. It contains volume-limited samples for G-type ($d_{lim} = 14$ pc), K-type ($d_{lim} = 12$ pc), and M-type ($d_{lim} = 6$ pc) stars with detection rates of more than 90%. The NEXXUS tables were kindly provided to us by the authors; they list M_V, $B - V$, and L_X in the 0.1–2.4 keV *ROSAT* band, and the X-ray surface flux F_X. We used the data for the 43 G-type stars (including 4 nondetections), the 54 K-type stars (including 2 nondetections), and the 79 M-type stars (including 5 nondetections). Bolometric luminosities, effective temperatures, and masses of the stars were estimated by interpolation using MS relationships of these quantities with the absolute magnitude M_V.

When comparing the NEXXUS data to our COUP data, one has to take into account the different energy bands for which X-ray luminosities were computed. The NEXXUS X-ray luminosities are given for the 0.1–2.4 keV *ROSAT* band, and for comparison with our COUP results we have to transform these luminosities into the 0.5–8 keV band. The transformation factor can be calculated with PIMMS and depends on the X-ray spectrum; since we can assume thermal plasma spectra, the transformation mainly depends on the plasma temperature. For the NEXXUS stars, the count rate to luminosity transformation factor used by Schmitt & Liefke (2004) assumes a plasma temperature of ~2.5 MK, and the corresponding energy band correction factor is 0.33 dex. In the following comparisons we also consider the X-ray properties of our Sun. For this, we use here the *ROSAT*-band X-ray luminosity range of $\log(L_X\ [\mathrm{ergs\ s^{-1}}]) = 26.8$–$27.9$ based on the results of Judge et al. (2003) for the activity range of a typical solar cycle. Assuming a plasma temperature of 2 MK, the flux in the 0.5–8 keV band is 0.48 dex lower than that in the 0.1–2.4 keV band.

Figure 6 compares the $L_X \leftrightarrow L_{bol}$ relations for the COUP optical sample to that for the NEXXUS sample of field stars. A clear correlation between X-ray and bolometric luminosity is seen not only for the ONC TTSs, but also for the NEXXUS field stars. The tests in ASURV show that the correlation for the NEXXUS

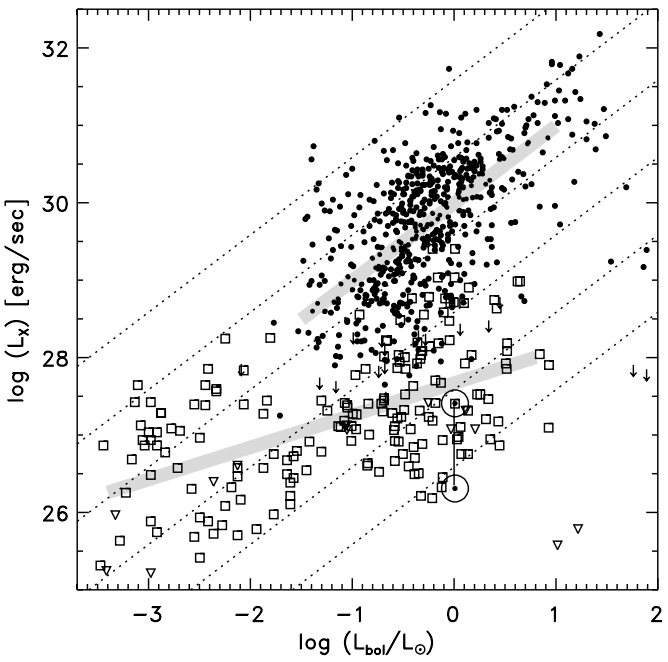

FIG. 6.—X-ray luminosity vs. bolometric luminosity for the stars in the COUP optical sample (*solid dots, arrows for upper limits*) and for the NEXXUS sample of nearby field stars (*open squares, triangles for upper limits*). The dotted lines mark $\log(L_X/L_{bol})$ ratios of -2, -3, -4, -5, -6, and -7. The thick gray lines show the linear regression fits with the EM algorithm computed with ASURV for these two samples.

stars is significant $[P(0) < 10^{-4}]$; the linear regression fit with the EM algorithm for the G-, K-, and M-type stars in the NEXXUS sample yields a power-law slope of 0.42 ± 0.05, which is much shallower than the slope found for the $L_X \leftrightarrow L_{bol}$ correlation for the COUP stars (1.04 ± 0.06).

Figure 7 compares the $L_X \leftrightarrow M$ relations for the COUP optical sample to that for the NEXXUS sample of field stars. It is interesting to see that there is a clear correlation between X-ray luminosity and mass for the NEXXUS field stars. The tests in ASURV show that the X-ray luminosity and mass are clearly correlated $[P(0) < 10^{-4}]$; the linear regression fit with the EM algorithm for objects in the mass range 0.08–2 $M_\odot$ yields $\log(L_X\ [\mathrm{ergs\ s^{-1}}]) = 27.58(\pm 0.07) + 1.25(\pm 0.15) \log (M/M_\odot)$ with a standard deviation of 0.77. The corresponding correlation for the TTSs in the COUP optical sample yielded a power-law slope of 1.44 ± 0.10, which is consistent with the slope for the field stars within the uncertainties. The similarity of the slopes found in the $L_X \leftrightarrow M$ relations for the ONC TTSs and the field stars may indicate that the relation between stellar mass and X-ray luminosity is more fundamental than that between bolometric and X-ray luminosity.

The plot of fractional X-ray luminosities against stellar masses (Fig. 7) shows that some of the very low mass field stars reach similar activity levels as the TTSs. The solar-mass field stars, on the other hand, are typically much less X-ray active than their young COUP counterparts. The different activity levels of the field stars as a function of mass can be understood as a consequence of the activity-rotation relation for MS stars: many of the very low mass field stars are rapid rotators and thus show high levels of X-ray activity, while most solar-mass field stars rotate quite slowly, therefore displaying lower activity levels. For the COUP stars, on the other hand, we show in § 5 that all stars with known rotation period rotate more rapidly than the Sun and that their X-ray activity is probably unrelated to their rotation period.

5. X-RAY EMISSION, ROTATION, AND CONVECTION

5.1. *The Activity-Rotation Relation for the TTSs*

For MS stars, the well-established correlation between fractional X-ray luminosity and rotation period (e.g., Pallavicini et al. 1981; Pizzolato et al. 2003) constitutes the main argument for a solar-like dynamo mechanism as the origin of their X-ray activity. As already noted in the introduction, the existence of a similar activity-rotation relation could not be unambiguously

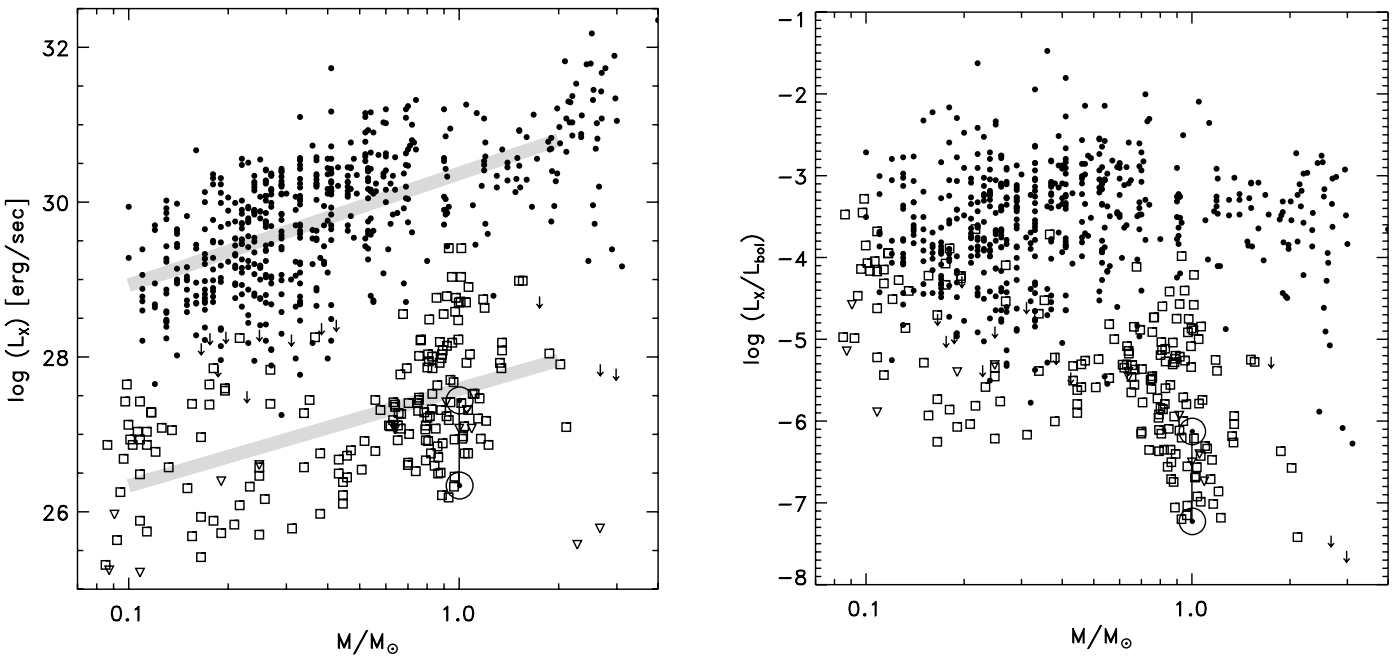

FIG. 7.—Absolute (*left*) and fractional (*right*) X-ray luminosity vs. stellar mass for the stars in the COUP optical sample (*solid dots, arrows for upper limits*) based on masses determined with the PMS models of Siess et al. (2000) and for the NEXXUS sample of nearby field stars (*open squares, triangles for upper limits*). The thick gray lines in the $L_X \leftrightarrow M$ correlation show the linear regression fits with the EM algorithm in ASURV for the low-mass ($M \leq 2\ M_\odot$) stars in these two samples.

proven for PMS stars, mainly due to a lack of statistical power in the underlying data (in most studies the sample sizes were too small for statistically significant conclusions to be drawn). The previous *Chandra* ONC studies (Feigelson et al. 2002a; Flaccomio et al. 2003b), however, provided strong evidence that the TTSs do *not* follow the activity-rotation relation for MS stars.

Table 9 in Getman et al. (2005a) lists rotation periods for 158 stars in our COUP optical sample. If we also consider the additional rotation data as listed in Flaccomio et al. (2005), rotation periods from photometric monitoring are available for 228 stars in our optical TTS sample (169 M-type stars, 58 K-type stars, and one G-type star). In Figure 8 we plot the fractional X-ray luminosity versus rotation period for these stars and compare them to data for MS stars. It is rather obvious that the COUP stars do not follow the well-established activity-rotation relation shown by the MS stars, i.e., increasing activity for decreasing rotation periods followed by saturation at $L_X/L_{bol} \sim 10^{-3}$ for the fastest rotators. A statistical analysis reveals for the COUP stars a correlation between L_X/L_{bol} and P_{rot} rather than the anticorrelation seen for the MS stars: the linear regression analysis with SLOPES (Isobe et al. 1990; Feigelson & Babu 1992) yields a bisector regression fit of the form $\log(L_X/L_{bol}) = -4.21(\pm 0.07) + 1.27(\pm 0.09) \log(P_{rot}\ [\mathrm{days}])$. This correlation is statistically significant; a Kendall's τ and Spearman's ρ test give probabilities of $P(0) = 0.0002$ for the null hypothesis that a correlation is not present. The observed correlation between L_X/L_{bol} and P_{rot} is clearly very different from the anticorrelation shown by the MS stars (where the bisector regression fit yields a slope of -2.35 ± 0.16 for the sample shown in Fig. 8 in the period range 1–10 days). These results do not change significantly if we use the characteristic rather than the average X-ray luminosities.

Before we consider possible explanations for these findings, it is important to note that rotation periods are known for only ~38% of the X-ray–detected stars in our optical sample and that this subsample may be biased with respect to its X-ray properties. Stassun et al. (2004a) studied archival ACIS data of the ONC and pointed out that the stars with known rotation period in their sample show systematically higher X-ray activity than the stars with unknown periods. A similar difference is present in our COUP optical sample: the median fractional X-ray luminosity for the TTSs with known rotation periods is at $\log(L_X/L_{bol}) = -3.31$, while the median value for TTSs with unknown periods is -3.71. A K-S test gives a probability of $P(0) \ll 10^{-4}$ for the hypothesis that the distributions of fractional X-ray luminosities in both samples are identical, i.e., the apparent difference of about a factor of ~2.5 in X-ray activity is statistically significant. This difference is not due to systematic differences in the basic stellar parameters[15] of the two samples.

The explanation of this difference was discussed in detail by Stassun et al. (2004a): Rotation periods can only be determined for stars showing sufficiently large spot-related photometric variability. The level of photometric variability, however, is related to the level of magnetic activity, and therefore the more active stars (i.e., those with higher X-ray luminosities) are easier targets for a determination of photometric rotation periods, while the less active stars (i.e., those with lower X-ray luminosities) show too small photometric variability to allow determination of periods. A quantitative description of these interrelations for the case of MS stars has been given by Messina et al. (2003). It is therefore likely that the COUP stars without known rotation periods rotate on average slower than the stars with known periods. This introduces a bias into our sample, since most of the missing stars (i.e., those without known rotation periods) have lower fractional X-ray luminosities and longer rotation periods than the stars in our sample. The apparent correlation between X-ray activity and rotation period may therefore (in part) be due to these selection effects.

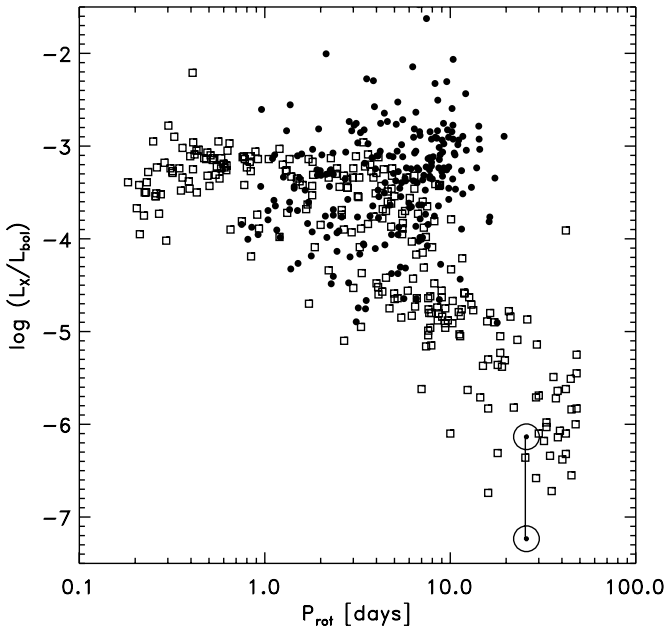

FIG. 8.—Fractional X-ray luminosity vs. rotation period. This plot compares the ONC TTSs (*solid dots*) to data for MS stars from Pizzolato et al. (2003) and Messina et al. (2003) (*open squares*) and the Sun.

Nonetheless, it appears very unlikely that the ONC TTSs follow the same rotation-activity relation as found for MS stars. First, we note that the effects of the bias due to unknown rotation periods appear much too small to transform the strong $L_X/L_{bol} \leftrightarrow P_{rot}$ anticorrelation of the MS stars into an apparent positive correlation. Second, the quite high fractional X-ray luminosities for most TTSs in the period range between ~7 and ~15 days, which are more than 1 order of magnitude higher than the typical values for MS stars, also indicate differences between the TTSs and the MS sample. In conclusion, we are confident that the ONC TTSs do not follow the same rotation-activity relation as seen in MS stars, but it remains unclear whether and how the X-ray activity of the TTSs is correlated to their rotation periods.

The inability to draw meaningful conclusions from our X-ray and rotation data may be due to the fact that the rotation period is perhaps the wrong variable to look at. Theoretical studies of the solar-like $\alpha - \Omega$ dynamos show that the dynamo number is not directly related to the rotation period, but to more complicated quantities such as the radial gradient of the angular velocity and the characteristic scale length of convection at the base of the convection zone. It can be shown that (with some reasonable assumptions) the dynamo number is essentially proportional to the inverse square of the Rossby number Ro (e.g., Maggio et al. 1987). The Rossby number is defined as the ratio of the rotation period to the convective turnover time τ_c, i.e., $\mathrm{Ro} \equiv P_{rot}/\tau_c$. For MS stars, the theoretical expectations are well confirmed: it is well

[15] We note that the stars with known periods have systematically higher masses [$\Delta \log(M) \sim 0.06$ dex, $P_{KS}(0) = 0.006$] than the stars without periods. According to the correlation between stellar mass and fractional X-ray luminosity established in § 4, this difference in stellar masses would, however, predict a difference in the activity level of only $\Delta \log(L_X/L_{bol}) \sim 0.02$ dex, much smaller than the observed 0.4 dex difference between stars with and without known periods. This effect therefore cannot explain the difference in the activity levels of stars with and without known periods.

established (e.g., Montesinos et al. 2001) that the stellar activity shows a tighter relationship to the Rossby number than to rotation period. The shape of the relation is similar to that of the activity-rotation relation: for large Rossby numbers, activity rises strongly as $L_X/L_{bol} \propto Ro^{-2}$ until saturation at $L_X/L_{bol} \sim 10^{-3}$ is reached around $Ro \sim 0.1$, which is followed by a regime of "supersaturation" for very small Rossby numbers, $Ro \lesssim 0.02$.

The convective turnover timescale is a sensitive function of the physical properties in the stellar interior and its determination requires detailed stellar structure models. Many studies of stellar activity therefore used semiempirical interpolations of τ_c-values as a function of, e.g., $B - V$ color. This may be appropriate for MS stars but seems to be insufficient for TTSs, which have a very different and quickly evolving internal structure.

5.2. *Computation of Convective Turnover Times for the TTSs*

For the computation of convective turnover times a series of stellar evolution models with masses ranging from 0.065 to 4.0 $M_\odot$ was computed with the Yale Stellar Evolution Code. The evolution was assumed to start at the stellar birth line, where stars initially become visible objects (Palla & Stahler 1993). All models used the parameters derived for the standard solar model, where the initial X, Z, and the mixing-length ratio were varied until a solar model at the solar age of 4.55 Gyr has the observed solar values of luminosity, radius, and Z/X (=0.0244; Grevesse et al. 1996). The model that best matched the solar properties[16] was that of $(X, Z)_{initial} = (0.7149, 0.0181)$ and the mixing-length ratio 1.7432. These values were then used for all stellar models.

A detailed discussion of the physics used in this study for the construction of stellar models can be found in Yi et al. (2001). The most important aspects are as follows: The solar mixture was assumed as given by Grevesse & Noels (1993). For $\log T > 4$, OPAL Rosseland mean opacities (Iglesias & Rogers 1996) were used, for $\log T < 4$ opacities from Alexander & Ferguson (1994). The OPAL EOS 2001 equation of state (Rogers et al. 1996) was used and the energy generation rates were set according to Bahcall & Pinsonneault (1992). Neutrino losses were taken following Itoh et al. (1989), and for the helium diffusion the values of Thoul et al. (1994) were used.

Since the dynamo action is believed to take place at the base of the convection zone, anchored in the radiative layers just below the convective interface, the convective turnover time of the deepest part of the convection zone is the most relevant in the evaluation of the Rossby number. Our knowledge of stellar convection is too limited to calculate "correct" convection turnover times, because the characteristic length scales, as well as the velocities, are not well known. Even when one decides to resort to the mixing-length approximation, there are still uncertainties: the mixing-length ratio is assumed to be the same for all stars with different masses and/or at different evolutionary stages, which is probably not fully correct. However, for the convection near the base of the convection zone where the temperature gradient is for all practical purposes adiabatic, the mixing-length approximation is known to provide an adequate description of convection at least in an average sense (Kim et al. 1996). For the characteristic timescale of convective overturn, the convective turnover time (i.e., the local mixing length divided by the local velocity) was calculated at each time step, which was determined at a distance of one-half the mixing length above the base of the surface convection zone[17] (Gilliland 1986; Kim & Demarque 1996). The convective turnover times were determined for the stars in the optical sample according to the model that represents their corresponding state in the H-R diagram, i.e., reproduces the (T_{eff}, L_{bol}) values. The resulting values are shown in Figure 9. Note that the convective turnover times of the TTSs are much larger (up to factors of $\sim$8) than those in MS stars and depend strongly on the effective temperatures and ages of the stars.

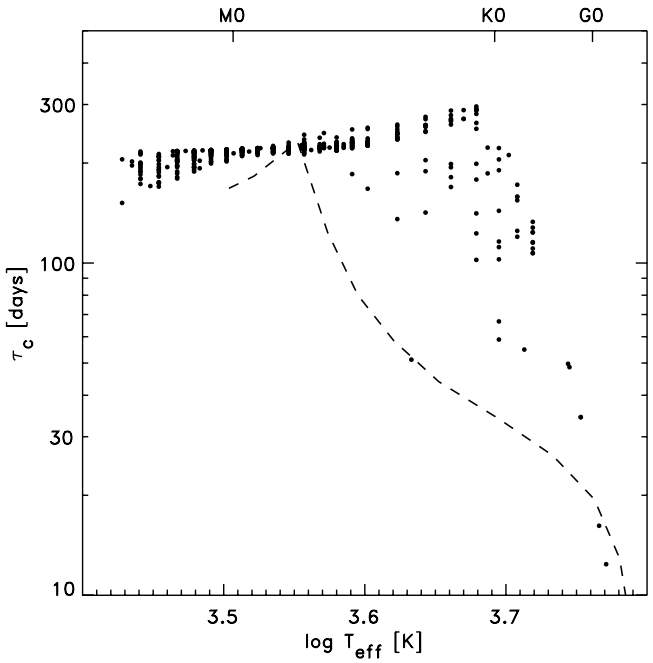

FIG. 9.—Local convective turnover time vs. spectral type for stars in the COUP optical sample (*solid dots*). The dashed line shows the local convective turnover times for stars 4.5 Gyr old.

5.3. *The Activity–Rossby Number Relation for the TTSs*

The Rossby numbers for the ONC TTSs were computed by dividing their rotation periods by the values for their local convective turnover time as derived above. The plot of fractional X-ray luminosity versus Rossby number in Figure 10 shows no strong relation between these two quantities. All TTSs have Rossby numbers <0.2 and therefore are in the saturated or supersaturated regime of the activity–Rossby number relation for MS stars. To search for indications of supersaturation, we compared the fractional X-ray luminosities of the TTSs in the saturated ($0.1 > Ro > 0.02$) and supersaturated ($Ro \leq 0.02$) regimes. Indeed, we found a slightly lower median $\log(L_X/L_{bol})$ value of -3.63 for the TTSs in the supersaturated regime as compared to -3.43 for those in the saturated regime; a K-S test gives a probability of $P(0) = 0.031$ for the assumption of equal L_X/L_{bol} distributions in both samples, i.e., the difference is significant at the 97% level. Thus, the fractional X-ray luminosities of the TTSs show a qualitatively similar relation to their Rossby numbers as is found for MS stars.

A remarkable difference between our TTS sample and the data for MS stars is the very wide dispersion of fractional X-ray luminosities at a given Rossby number in our TTS data. The scatter extends over about 3 orders of magnitude, and even if we

[16] We note that new precision measurements of elemental abundances on the solar surface imply a lower metallicity than previously assumed and lead to inconsistencies in theoretical solar models with respect to the depth of the solar convection zone (see Bahcall et al. 2004 and references therein).

[17] Note that for fully convective stars the base of the convection zone is the center.

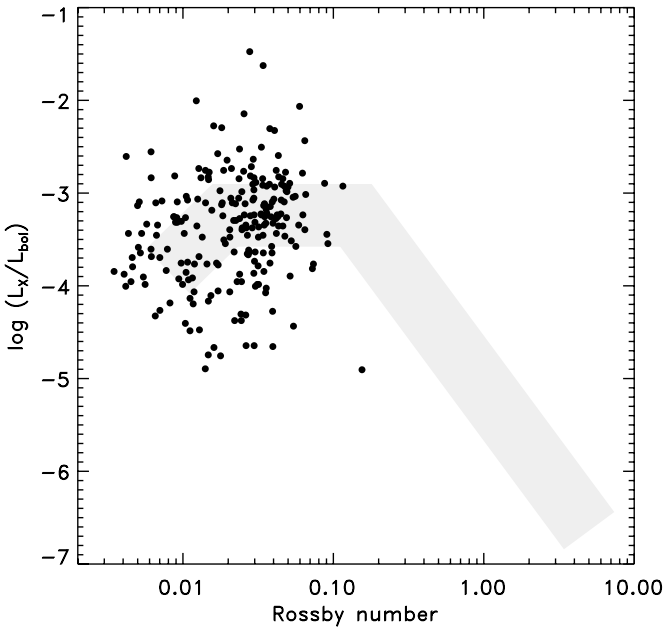

FIG. 10.—Fractional X-ray luminosity vs. Rossby number for the COUP stars. The gray shaded area shows the relation and the width of its typical scatter found for MS stars (from Pizzolato et al. 2003).

consider the characteristic (i.e., flare-cleaned) rather than the average X-ray luminosities, the scatter is only very slightly smaller. This large scatter is in strong contrast to the tight relation found for MS stars, where the scatter in $\log(L_X/L_{bol})$ at a given Rossby number is only about ± 0.5 dex (e.g., Pizzolato et al. 2003).

To conclude, we find that the X-ray activity of the ONC TTSs may depend on Rossby numbers in a similar way to what is found for MS stars, but the large scatter of X-ray activity at any given Rossby number suggests that additional factors are important for the level of X-ray activity.

6. POSSIBLE EXPLANATIONS FOR THE WIDE SCATTER IN THE CORRELATIONS

All the correlations between the X-ray activity and other stellar parameters show a very large scatter, often exceeding 3 orders of magnitudes. Three obvious reasons for the presence of scatter are uncertainties in the variables, X-ray variability, and unresolved binaries. Can these effects account for the wide scatter seen in the correlations? We first consider X-ray variability.

Most of the COUP sources show strong variability in their light curves. It is well known that variability is a common feature in the X-ray emission from TTSs, active stars, and also our Sun. The degree of variability is a function of the timescales. For active MS stars and the Sun, short-term variability (timescales of minutes to hours) is usually dominated by flares, which can cause large variations (sometimes exceeding factors of 10). On timescales from days to weeks, the typical variations are about a factor of 3 and up to 10, while the typical variability on timescales from months to years is a factor of about 3–4 (e.g., Micela & Marino 2003; Orlando et al. 2004). Furthermore, indications for stellar X-ray activity cycles have been found for some stars; these cycles can induce more than 1 order of magnitude of variability over a few years (e.g., Favata et al. 2004).

In previous, generally much shorter X-ray observations of TTSs, the large scatter was often assumed to be probably due in part to X-ray flaring. The COUP data provide two important pieces of information in this respect. First, the influence of individual flares on the average X-ray luminosity is strongly smoothed out by the long time basis of the COUP observation; the scatter seen in the correlations based on our COUP data should therefore be much smaller than what would be found from shorter, snapshot-like observations. Second, the use of the characteristic X-ray luminosities, which effectively exclude periods of flaring from the light curves, should further reduce the scatter, if short-term X-ray variability were the main reason for the large scatter in the correlation diagrams. These expectations are, however, not confirmed in our data: We find that the scatter in the COUP (i.e., 10 day average) X-ray luminosities of the ONC TTSs, e.g., as a function of bolometric luminosity or mass, is very similar to that found in the correlations based on the previous 23 hr ACIS observation (Feigelson et al. 2002a). Also, the use of characteristic rather than average X-ray luminosities reduces the scatter only marginally. This suggests that variability on timescales between $\sim$1 and $\sim$10 days is *not* the main source of the large scatter in the correlations between X-ray activity and other stellar parameters.

What about variability on longer timescales? We can investigate the variations on timescales of several years by comparison of the COUP data (obtained in 2003 January) to the previous 23 hr ACIS observations of the ONC (obtained in 1999 October and 2000 April) given by Feigelson et al. (2002a). For 515 of the COUP-detected stars in our optical sample X-ray luminosities based on the 23 hr observations are listed by Feigelson et al. (2002a). Since the spectral fitting procedure used in the analysis of the 23 hr data is not identical to that used for the COUP data, we compare here the *observed* X-ray luminosities, L_t, without extinction correction, which just give the integral of the observed flux over the spectrum. We find a good agreement of the luminosities from the two observations separated by more than 3 yr: the median absolute deviation from equal luminosities is only 0.31 dex, corresponding to just a factor of $\sim$2. This demonstrates that the X-ray luminosities of most ONC TTSs vary only slightly on timescales of several years. The observed level of variability cannot account for the large scatter seen in the correlation diagrams.

Now we try to quantify the uncertainties of the variables in the correlation diagrams. According to H97, the uncertainties in $\log L_{bol}$ are $\sim$0.2 dex. The uncertainties in the stellar mass estimates are probably of a similar magnitude. The uncertainties of the X-ray luminosities, derived from the spectral fits, are difficult to determine because the spectral models are highly nonlinear and the individual spectral parameters are often strongly correlated. Furthermore, ambiguities can occur when two qualitatively different spectral models give similarly good fits. We therefore assume the typical random uncertainties of $\log L_X$ to be similar to the uncertainties in the emission measures derived in the spectral fits, i.e., about 0.15 dex. Note, however, that some sources may be affected by systematic errors, which may well exceed this level.

Finally, we consider the effect of unresolved binaries. The presence of an unresolved companion causes an overestimation of both the bolometric and the X-ray luminosity. However, if X-ray and bolometric luminosity are related linearly (as our data suggest), unresolved companions should only shift the position of a star in the $L_X \leftrightarrow L_{bol}$ diagram along the correlation line and not increase the scatter. The stellar mass determined by comparison with PMS tracks depends (in the case of low-mass stars) mainly on the measured spectral type; as the combined optical spectrum of a binary system is dominated by the light of the primary component, the inferred mass is that of the primary,

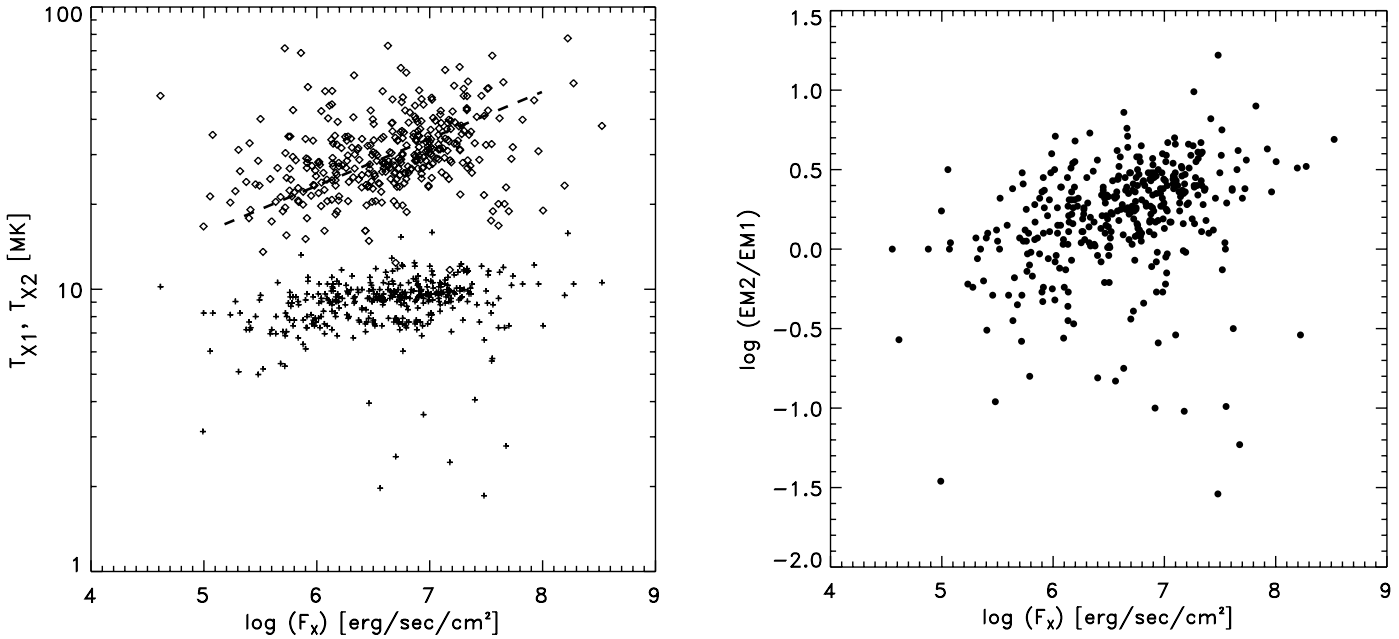

FIG. 11.—*Left*: Plasma temperatures (T_{X1}, *crosses*; T_{X2}, *diamonds*) derived in the X-ray spectral fits for the TTSs in the COUP optical sample plotted vs. the X-ray surface flux. The dashed line shows the relation $F_X \propto T^6$. *Right*: Emission measure ratio of hot and cool plasma components vs. the X-ray surface flux.

whereas the observed X-ray luminosity is the sum for primary and companion. If X-ray luminosity and stellar mass are correlated, the overestimation of the X-ray luminosity should be at most a factor of 2;[18] the typical shift in $\log L_X$ depends on the distribution of mass ratios in the binary systems (which is not well known) but is presumably about 0.2–0.3 dex among the low-mass stars.

The combined effect of the variability, the uncertainties in the variables, and unresolved binaries should therefore produce a scatter of roughly $\pm$(0.4–0.5) dex. This is considerably less (by about a factor of 2) than the scatter observed in the correlation diagrams, where the standard deviations are typically $\sim$0.7 dex. A large fraction of the scatter in the correlations must therefore be due to other reasons, most likely due to intrinsic differences in the X-ray activity levels of the TTSs. In § 8 we will show that the large scatter is probably related to the influence of accretion on the X-ray properties.

7. X-RAY PLASMA TEMPERATURES

As described in Getman et al. (2005a), the X-ray spectra of the COUP sources were fitted with single-temperature or (in most cases) two-temperature thermal plasma models plus absorption. We are fully aware that these relatively simple models are not "perfect," since it is well known that the coronae of active stars are generally not monothermal and can usually not be considered as to consist of just two different temperature components (e.g., Brickhouse et al. 2000; Sanz-Forcada et al. 2003). Nevertheless, this approach is justified because the purpose of our analysis was to characterize the coronal temperatures of the COUP stars in a homogenous way using a parsimonious model, rather than to perform a detailed investigation of the temperature structure of those sources (which will be the topic of separate studies). As demonstrated, for example, by Peres et al. (2004), fits of simulated spectra based on continuous temperature distributions with simple one- or two-temperature models usually yield temperatures near the peaks of the underlying temperature distribution. We therefore assume that the temperatures derived from the fits reflect some kind of a "characteristic" temperature, which then can be related to other stellar parameters.

In Figure 11 we plot the plasma temperatures and the ratios of the emission measures of the hot and cool component derived in the spectral fits versus the X-ray surface flux. First, we note that the temperature of the hot plasma component increases

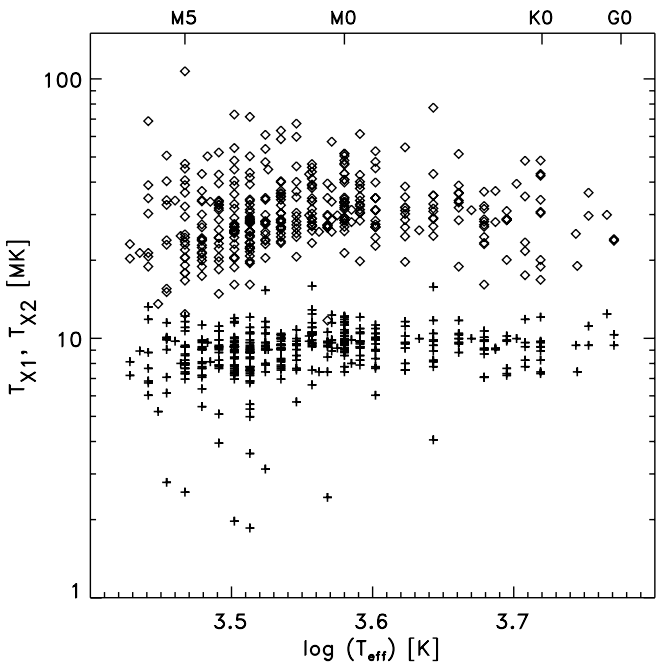

FIG. 12.—Plasma temperatures (T_{X1}, *crosses*; T_{X2}, *diamonds*) derived in the X-ray spectral fits for the TTSs in the COUP optical sample plotted vs. the effective temperature.

[18] There may, however, be larger effects in special cases. For example, in the case of a binary system in which both components show very different amounts of extinction, a fit to the combined X-ray spectrum may easily lead to wrong parameters.

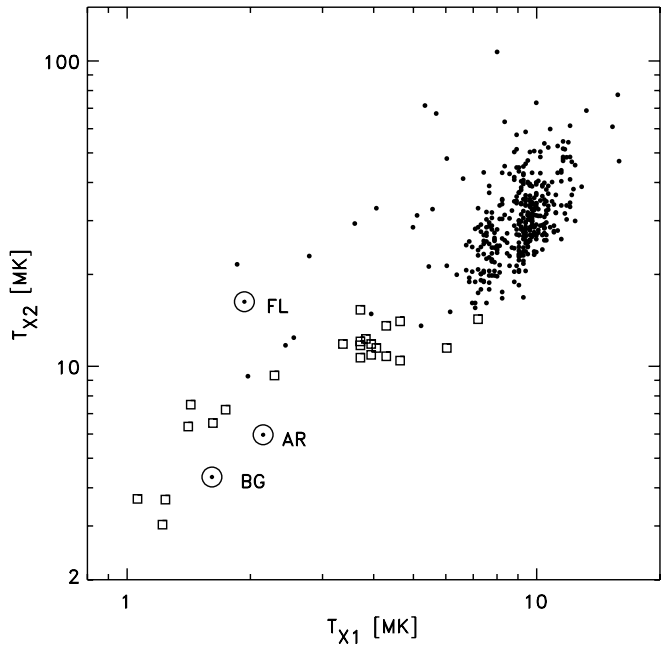

FIG. 13.—Temperature of the hot vs. the cool plasma component for the TTSs in the COUP optical sample (*solid dots*). The open squares show plasma temperatures derived for G- and K-type MS stars (Briggs & Pye 2003; Pillitteri et al. 2004; Güdel et al. 1997), and typical values for structures in the solar corona are also shown (BG = background corona; AR = active region; FL = flare; from Orlando et al. 2004).

with increasing surface flux; the slope is consistent the relation $F_X \propto T^6$, what is similar to a scaling relation derived for the solar corona by Peres et al. (2004) (which, however, was established for a much lower temperature range than that seen here on the TTSs). Second, we note that the relative contribution from the hot component (as measured by the ratio of emission measures for the hot and cool components) also increases with increasing X-ray activity. The most interesting result from these plots is the remarkable similarity of the temperatures of the cool plasma component in our sample. For nearly all stars a temperature of about 10 MK is found for the cool component. This suggests that this 10 MK component is a real feature in the coronal temperature distribution of the TTSs. It is interesting to note that a $\sim$10 MK plasma component seems to be some kind of a general feature of coronally active stars; for example, Sanz-Forcada et al. (2003) determined the emission measure distribution of 28 coronally active nearby field stars and found a peak at 8–10 MK in most of their stars. They argued that this temperature component may define a fundamental coronal structure, which is probably related to a class of compact loops with high plasma density.

Figure 12 shows the derived plasma temperatures as a function of stellar effective temperature. Among the M-type stars one can see a decrease in the temperature of the hot component for decreasing effective temperature. This can be understood as a consequence of the correlation of the hot plasma temperature with the level of X-ray activity (as traced by F_X or L_X/L_{bol}) and the decrease of X-ray activity with decreasing mass or effective temperature (see, e.g., Fig. 5).

In Figure 13 we plot the temperature of the hot versus that of the cool plasma component for the ONC TTSs. We also have included temperatures derived for G- and K-type stars in several young clusters and for solar-like field stars, as well as values for different structures in the solar corona as derived in the simulations of the "Sun as a star" by Orlando et al. (2004). The ONC TTSs follow the general correlation between the temperatures of the hot and cool plasma components seen for the MS stars, although nearly all TTSs show much higher temperatures than found on the MS stars. In the solar corona and in many active MS stars, plasma temperatures significantly exceeding 10 MK are only seen during strong flares. The high plasma temperatures found for the TTSs may suggest an increased contribution of flares to the total X-ray emission.

8. X-RAY EMISSION AND CIRCUMSTELLAR ACCRETION DISKS

It is still unclear how the (magnetic) interactions between a young stellar object and its surrounding circumstellar accretion disk influence the X-ray activity. Many X-ray observations of star-forming regions have been used to search for differences in the X-ray properties of the CTTSs [usually defined by the presence of Hα emission with equivalent widths $W(\mathrm{H}\alpha) \geq 10$ Å], which are thought to be actively accreting via circumstellar disks, and the WTTSs [$W(\mathrm{H}\alpha) < 10$ Å], which seem to lack disks and active accretion. The results of these investigations showed confusing differences: some studies (e.g., Gagné et al. 1995; Feigelson et al. 1993; Casanova et al. 1995; Preibisch & Zinnecker 2002) found no significant differences between the X-ray luminosity functions of CTTSs and WTTSs, while other studies, most notably the Taurus-Auriga study by Stelzer & Neuhäuser (2001), found clear differences in the X-ray luminosity functions, with the WTTSs being the stronger X-ray emitters. The two *Chandra* studies of the ONC before COUP also yielded seemingly contradictory results: Feigelson et al. (2002a) found no differences in the X-ray activity levels of stars with and without disks, whereas Flaccomio et al. (2003b) reported a strong difference in the X-ray activity levels of accreting and nonaccreting stars.

It is important to note that the different studies used different criteria to define the samples of CTTSs and WTTSs: sometimes the strength of the Hα or Ca emission line was used, while other studies used the presence or absence of near-infrared excess emission. These different kinds of indicators actually measure different things that cannot be directly compared: Hα or Ca line emission is thought to be a tracer of accretion, while infrared excess emission is a tracer of circumstellar material. While accretion obviously requires the presence of circumstellar material, the presence of circumstellar material alone does not necessarily mean that the young stellar object is also accreting. Furthermore, this issue is easily affected by strong selection effects if the samples of TTSs are either X-ray selected or based on optical selection criteria such as emission lines or infrared excess. For example, in many star-forming regions Hα emission was used as a tracer to find and define the population of T Tauri stars. This can easily introduce a strong bias, because the CTTSs are quite easy to recognize by their prominent Hα emission even if they are very faint, whereas WTTSs of similar brightness are much harder to identify. The optical Hα selected samples of TTSs are therefore often very incomplete for WTTSs and much more complete for the CTTSs (see discussion in Preibisch & Zinnecker 2002). In fact, the majority of WTTSs in many star-forming regions have been found through X-ray observations (cf. Neuhäuser 1997) and therefore suffer from an X-ray selection bias.

The COUP study provides us with the important advantage that we can use a statistically complete sample of all optically visible stars in the region, which does not suffer from any of the selection effects described above. In the following we will investigate how and in which way the X-ray activity is related to infrared excess emission as a tracer of circumstellar material

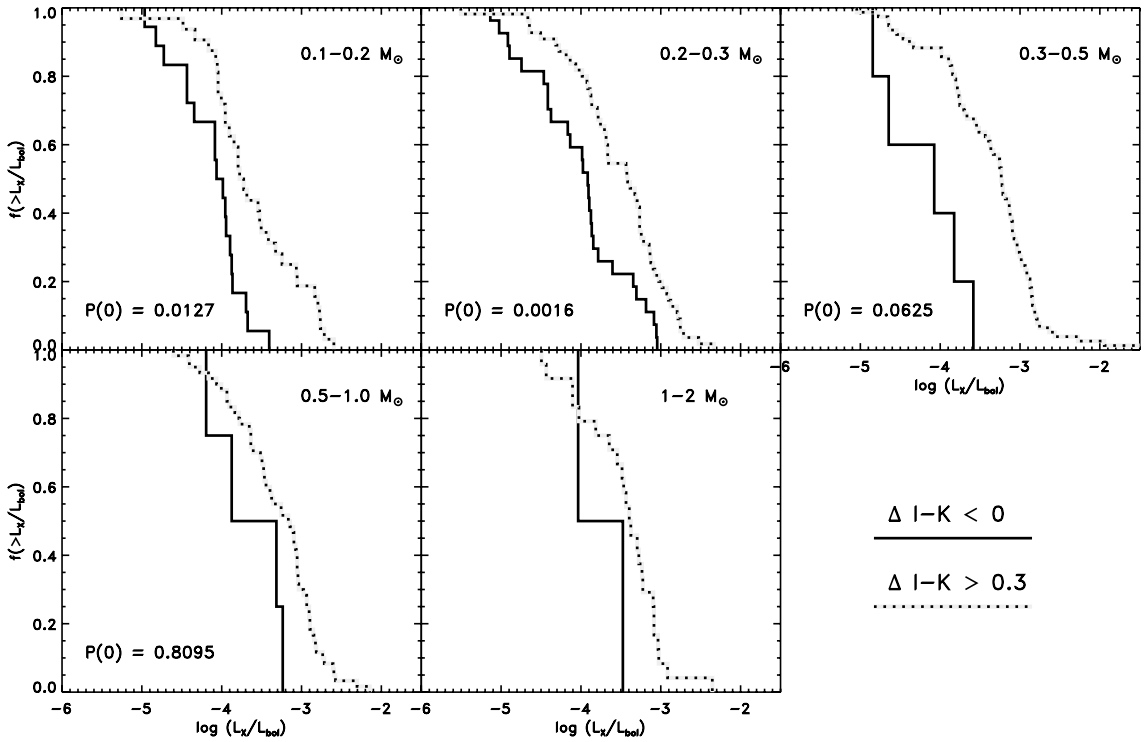

FIG. 14.—Cumulative distributions of the fractional X-ray luminosities for TTSs with [$\Delta(I-K) > 0.3$] and without [$\Delta(I-K) < 0$] infrared excess in the lightly absorbed optical sample for five different mass ranges. The K-S test probabilities for the assumption that both samples are drawn from the same underlying distribution are given in the lower left edge of each plot.

(§ 8.1), optical line emission as a tracer of accretion (§ 8.2), and estimates of accretion rates and luminosities from astrophysical models (§ 8.3).

8.1. *X-Ray Activity and Infrared Excess (=Inner Disk Tracer)*

A good way to discern between TTSs with and without circumstellar material is to look for infrared excess emission. The COUP tables list the color excess $\Delta(I-K)$ as determined by Hillenbrand et al. (1998). This quantity represents the color excess relative to the expected photospheric colors for the star's spectral type after correction for reddening due to extinction and has been shown to be a useful tracer of circumstellar material (see discussion in Hillenbrand et al. 1998). However, the $\Delta(I-K)$ excess is not optimal for detecting circumstellar material, since the K-band excess traces only the hottest dust in the innermost regions near the central star; it has been shown (e.g., Haisch et al. 2001) that many stars with circumstellar material show significant excess emission only at longer wavelengths. We therefore also used the L-band photometric data listed in the COUP tables and determined a color excess $\Delta(K-L)$ in an analog way as $\Delta(I-K)$. The $\Delta(K-L)$ excess has the advantage of being more sensitive for circumstellar material and less strongly affected by uncertainties in the visual extinction, but the disadvantage of being available for fewer (228) TTSs than $\Delta(I-K)$ (446 TTSs) in the optical sample.

Since the infrared excess emission in our sample is correlated to effective temperature and stellar mass, we compare in Figures 14 and 15 stars with and without excesses in mass-stratified samples. In the samples based on $\Delta(I-K)$ excess, we find significantly different [$P(0) < 0.02$] fractional X-ray luminosity distributions for the 0.1–0.2 $M_\odot$ and 0.2–0.3 $M_\odot$ bins, whereas for the more massive stars the differences are only of marginal statistical significance. If we use the $\Delta(K-L)$ excess (which we regard as more reliable), no significant differences are found for any of the mass ranges considered.

8.2. *X-Ray Activity and* Ca II *Line Emission (=Accretion Tracer)*

Next we consider the presence/absence of signs for active accretion rather than disks. We follow the strategy of Hillenbrand et al. (1998), who used the equivalent width of the 8542 Å Ca II line as an indicator of disk accretion. As they noted, stars without or with very weak accretion are expected to show this line in absorption with W(Ca II) ~ 3 Å and a rather weak dependence on the spectral type. In more strongly accreting stars, the line gets filled and the equivalent width should be related to the mass accretion rate. In their analysis of the *Chandra* HRC data of the ONC, Flaccomio et al. (2003b) classified stars as strong accretors if their Ca II line is in emission and has an equivalent width of W(Ca II) < -1 Å, while stars with the Ca II line in absorption with W(Ca II) > 1 Å are assumed to be not (or at most very weakly) accreting. Using this scheme, 142 (136) of the objects in our (lightly absorbed) optical sample are classified as strong accretors, and 134 (123) objects are classified as weak or nonaccretors. In the following text, we will simply denote these two groups as "accretors" and "nonaccretors."

Flaccomio et al. (2003b) found a clear difference in the (fractional) X-ray luminosities of the accretors and nonaccretors in their *Chandra* HRC data of the ONC, with the accretors being considerably (about a factor of 2–3) less X-ray bright than the nonaccretors. A similar, although less pronounced, effect is found in our COUP data. In Figure 16 we show the distributions of fractional X-ray luminosities of accreting and nonaccreting stars in different mass bins. A significant difference between accretors and nonaccretors is only found for the 0.3–0.5 $M_\odot$ stars, whereas the other mass ranges show only marginal or no evidence at all for a difference in the distribution functions of fractional X-ray luminosities.

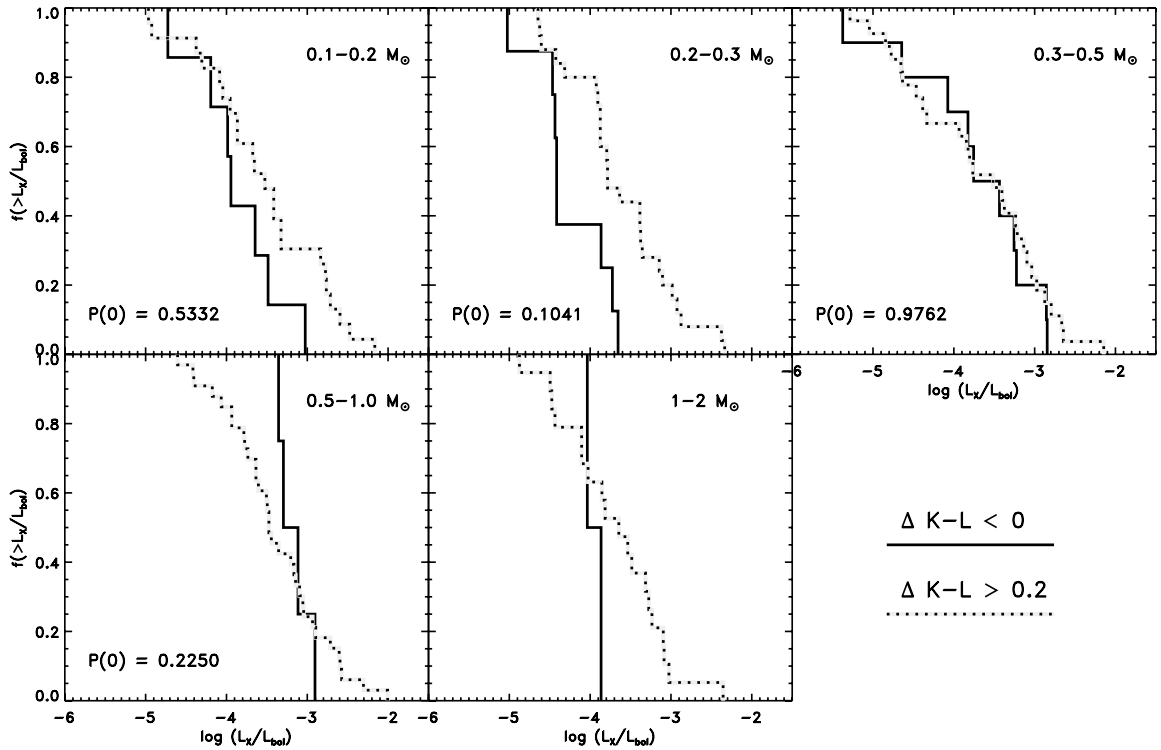

FIG. 15.—Cumulative distributions of the fractional X-ray luminosities for TTSs with $[\Delta(K-L) > 0.2]$ and without $[\Delta(K-L) < 0]$ infrared excess in the lightly absorbed optical sample for five different mass ranges. The K-S test probabilities for the assumption that both samples are drawn from the same underlying distribution are given in the lower left edge of each plot.

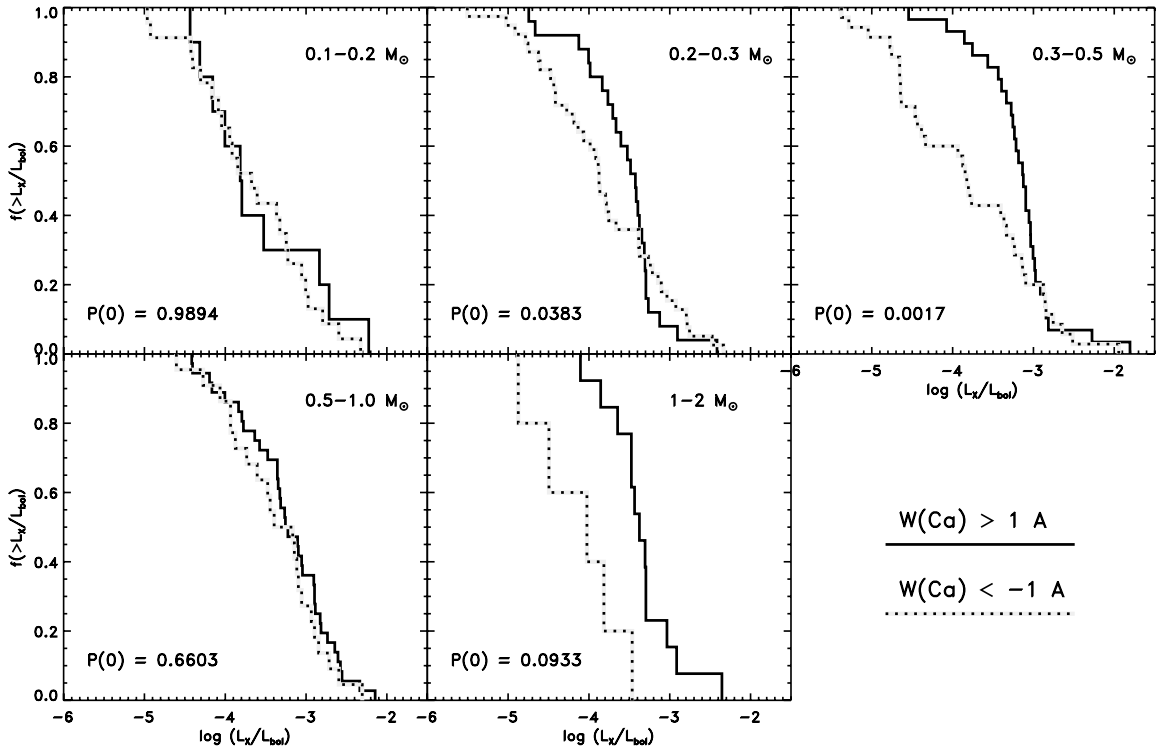

FIG. 16.—Cumulative distributions of the fractional X-ray luminosities for accreting and nonaccreting TTSs in the lightly absorbed optical sample for five different mass ranges. The K-S test probabilities for the assumption that both samples are drawn from the same underlying distribution are given in the lower left edge of each plot.

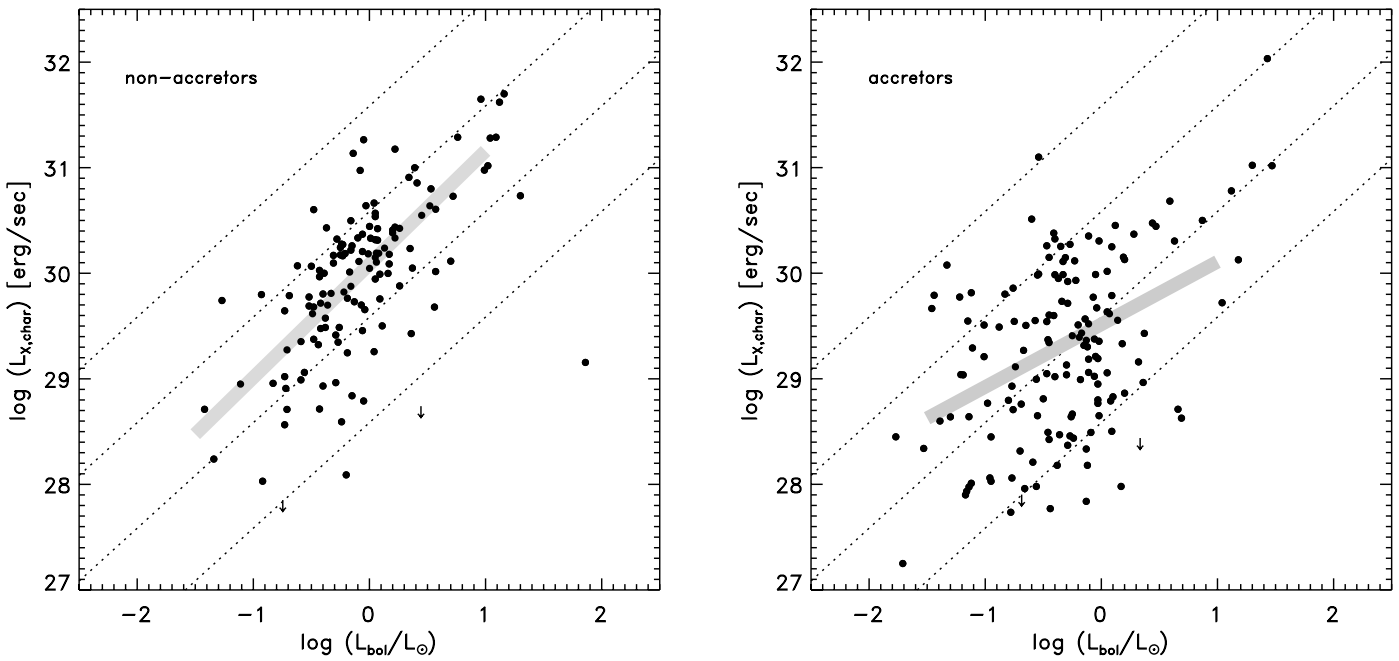

FIG. 17.—Characteristic X-ray luminosity vs. bolometric luminosity for the stars in the optical sample with the 8542 Å Ca II line in absorption (*left*, nonaccretors) and in emission (*right*, accretors). The dotted lines mark $\log(L_X/L_{bol})$ ratios of -2, -3, -4, and -5. The thick gray lines show linear regression fits for $L_{bol} \leq 10\ L_\odot$ stars with the EM algorithm computed with ASURV.

To investigate the difference between accreting and nonaccreting stars further, we compare in Figure 17 the correlations between characteristic X-ray luminosities and the bolometric luminosities for the nonaccretors and the accretors. The nonaccretors show a very well-defined correlation between $L_{X,\,char}$ and L_{bol}, and the linear regression fit with the EM algorithm gives a power-law slope 1.1 ± 0.1 and standard deviation of 0.52 dex in $\log L_{X,\,char}$. For the accretors, the correlation is much less well defined; the linear regression fit with the EM algorithm gives a power-law slope 0.6 ± 0.1 and standard deviation of 0.72 dex in $\log L_{X,\,char}$. Very similar results are found for the correlations between characteristic X-ray luminosities and stellar masses for the nonaccretors and the accretors.

As discussed in § 6, the scatter in the correlations due to X-ray variability, the uncertainties in the variables, and unresolved binaries is expected to be about 0.4–0.5 dex. The standard deviation found for the $L_X \leftrightarrow L_{bol}$ correlation (or the $L_X \leftrightarrow M$ correlation) for the nonaccreting stars agrees well to that expectation, whereas the accreting stars show a considerably larger scatter. Some fraction of this scatter may be due to the fact that the more rapidly accreting stars may have larger errors compared to nonaccreting stars in stellar luminosity and effective temperature values due to the effects of accretion on the observables that lead to these quantities.

Another important result is found when considering the mean fractional X-ray luminosities: For the nonaccretors, the median value for $\log L_X/L_{bol}$ is -3.31, which is in very good agreement to the mean saturation value for rapidly rotating low-mass (0.22–0.6 $M_\odot$) field stars derived by Pizzolato et al. (2003). This means that the fractional X-ray luminosities of the nonaccreting TTSs are consistent with those of much older coronally active field stars. For the accretors, on the other hand, we find a median value for $\log(L_X/L_{bol})$ of -3.74, which is a factor of about 3 lower than the saturation value for fast-rotating low-mass field stars. The accreting TTSs therefore are responsible for the "X-ray deficit" of the ONC TTSs, i.e., the fact that the median fractional X-ray luminosity of the TTSs is lower than that found for rapidly rotating MS stars.

We also looked for possible relations between the X-ray activity and the rotation rates of the accretors and nonaccretors. The rotation periods found for the nonaccretors and accretors overlap strongly, but the nonaccretors show shorter median periods (3.8 days) than the accretors (6.8 days); a K-S test gives a probability of only 0.03 that the distribution of periods is identical in both groups. However, neither for the accretors nor for the nonaccretors are statistically significant correlations found between activity and rotation. The median fractional X-ray luminosities of the nonaccretors and accretors with known rotation period are nearly identical, -3.3 ± 0.4 and -3.4 ± 0.8. The difference in X-ray activity between accreting and nonaccreting stars described above thus cannot be explained by differences in their rotation periods or their rotation-activity relations. Considering the relation between X-ray activity and Rossby numbers, we also find no significant correlations for either accretors or nonaccretors.

8.3. *X-Ray Activity and Accretion Rates/Luminosities*

Robberto et al. (2004) recently determined accretion rates and accretion luminosities for a sample of 40 TTSs in the Trapezium cluster from *Hubble Space Telescope U*- and *B*-band photometry. As the computation of the accretion parameters from the UV excess is quite indirect and involves numerous assumptions, their values have considerable uncertainties; for some of their stars they find even negative values for the accretion luminosities. We therefore restrict ourselves to those 30 stars for which they derived positive values for the accretion luminosity and note that 29 of these are detected as X-ray sources in COUP.

For a considerable fraction of these objects the X-ray luminosities are comparable or even larger than the accretion luminosities; this is a strong argument against the assumption that the X-ray emission in these TTSs is directly created in the accretion process (e.g., comes from the accretion shock; see discussion below). Furthermore, we find a weak anticorrelation of

the fractional X-ray luminosity with accretion rate (and also with accretion luminosity); although these correlations are not statistically significant, they agree to the above results based on the Ca line width classification and suggest that active accretion somehow lowers the X-ray activity levels.

8.4. *Summary of the Relations between X-Ray Activity and Accretion*

We find that the TTSs with inner circumstellar material as traced by near-infrared excess show slightly higher fractional X-ray luminosities than the TTSs without near-infrared excess, but this difference is of only marginal statistical significance. Using the equivalent width of the Ca II line to discern between accreting and nonaccreting stars, we find that the nonaccretors show very well-defined correlations between X-ray luminosity and bolometric luminosity or stellar mass. The accreting stars, on the other hand, produce much poorer correlations between L_X and L_{bol} or stellar mass and much more scatter. Furthermore, the mean fractional X-ray luminosities of the nonaccreting TTSs are well consistent with those of rapidly rotating MS stars, while the accreting TTSs show levels of X-ray activity about 3 times lower. Finally, we have shown that X-ray activity appears to be anticorrelated with mass accretion rate. In conclusion, the X-ray activity of the nonaccreting TTSs is consistent with that of rapidly rotating MS stars, while in accreting TTSs the X-ray emission is somehow suppressed.

9. IMPLICATIONS ON THE ORIGIN OF TTS X-RAY EMISSION

In this section we summarize the implications we can derive from our X-ray data on the origin of the observed X-ray emission from the TTSs. We consider the following questions: Where is the X-ray–emitting plasma located? What is the reason for the lower X-ray activity of accreting stars in comparison to nonaccretors? What is the ultimate origin of the magnetic activity, and what kind of dynamo may work in the TTSs?

9.1. *Location of the X-Ray–Emitting Structures*

9.1.1. *X-Ray Emission from Accretion Shocks?*

According to the magnetospheric accretion scenario, accreted material crashes onto the stellar surface with velocities of up to several 100 km s^{-1}, which should cause hot ($\lesssim 10^6$ K) shocks in which strong optical and UV excess emission and perhaps also soft X-ray emission is produced (e.g., Lamzin et al. 1996; Calvet & Gullbring 1998). The expected characteristics of X-ray emission from accretion shocks would be a very soft spectrum (due to the low plasma temperature in the shock of at most a few MK), and perhaps simultaneous brightness variations at optical/UV wavelengths and in the X-ray band. Although earlier studies failed to find evidence for this scenario (e.g., Gullbring et al. 1997), more recent high-resolution X-ray spectroscopy of *some* TTSs (e.g., TW Hya, XZ Tau, and BP Tau; see Kastner et al. 2002; Stelzer & Schmitt 2004; Favata et al. 2003; Schmitt et al. 2005) yielded plasma temperatures and densities that have been interpreted as evidence for X-ray emission originating from a hot accretion shock.

The COUP results provide no support for a scenario in which X-ray emission is dominated by accretion power. First, we note that many of the accreting TTSs show X-ray luminosities considerably larger than their total accretion luminosities. Although we have to be somewhat cautious because the X-ray and accretion rate measurements were not simultaneous and accretion is thought to be strongly time variable, it appears extremely unlikely that the bulk of the observed X-ray emission from the TTSs could originate from accretion processes.

Second, the COUP spectra of nearly all TTSs show much higher plasma temperatures (typically a $\sim$10 MK cool component and $\gtrsim$20 MK hot component) than the $\lesssim$1–3 MK expected from shocks for the typical accretion infall velocities. For only five of the TTSs in our optical sample the X-ray spectral fits yielded plasma components with temperatures below 3 MK. No accretion rates for these stars are known, only two of them show Ca II emission, and only one displays infrared excess. Thus, we cannot determine whether in any of these objects the X-ray emission may be related to accretion shocks. We just note that the low plasma temperatures alone provide no evidence for an accretion shock origin of the X-rays, since similarly low (or even lower) plasma temperatures are found for MS stars and the Sun, i.e., for stars that are certainly not accreting. Furthermore, the COUP light curves show thousands of high-amplitude flares whose temporal structure closely resembles solar-type magnetic flares and is very unlikely to be reproduced by thermal accretion shocks. Indeed, Stassun et al. (2005) have compared these COUP light curves with simultaneous optical light curves and find very little evidence to suggest that X-ray variability is correlated with accretion-related processes.

Of course, these arguments do not exclude the possibility that accretion shocks may contribute *some fraction* of the X-ray emission in TTSs. It is critical to note that *Chandra*'s ACIS-I instrument is not very sensitive to the cooler plasma expected from these accretion shocks, and much of this emission may be attenuated by line-of-sight interstellar material. We note that evidence for a scenario of mixed X-ray emission in accreting YSOs has recently come from an X-ray high spectral resolution observation of BP Tau (Schmitt et al. 2005), where hot plasma (too hot to be shock-produced and thus likely magnetically confined and heated in some form of coronal structure) coexists with cool (1–3 MK) plasma for which unusually high densities were inferred, which may be well explained by accretion shock models.[19]

We conclude that, although accretion shock emission must be present, plays an important role in optical or ultraviolet emission of CTT stars (e.g., Lamzin et al. 1996), and may contribute some fraction of the largely unobserved soft X-ray emission of TTSs, it is not responsible for the bulk of the X-ray emission seen in the COUP data.

9.1.2. *X-Ray Emission from Magnetic Star-Disk Interactions?*

Another possibility for a non–solar-like origin of the X-ray radiation may be plasma trapped in magnetic fields that connect the star with its surrounding accretion disk. The dipolar stellar magnetic field lines anchored to the inner part of the accretion disk should be twisted around because of the differential rotation between the star of the disk. Theoretical work suggests that the twisted field lines periodically reconnect, and the released magnetic energy heats plasma trapped in the field lines

[19] The cool plasma in BP Tau shows a very low value of the ratio between the intensity of the forbidden and intercombination lines ($R = f/i$) for the O VII triplet, formed at temperatures of 1–3 MK. Low R-values (also observed in TW Hya, and in no coronal source) can either imply very high densities, or the presence of an intense UV field, as indeed expected within the accretion spot. Too high densities would, however, be difficult to explain given the pressure structure of an accretion shock (see Drake 2005) in which the plasma at $n_e \simeq 10^{13}$ cm^{-3} (the density implied by the R value observed in TW Hya) is buried (following, e.g., the shock structure and emission models by Calvet & Gullbring 1998) under a column density of typically $\gtrsim 10^{22}$ cm^{-3}, that should absorb the soft X-ray emission from the shock zone nearly completely and thermalize the high-energy radiation within or close to the shock.

to very hot, X-ray–emitting temperatures (Hayashi et al. 1996; Montmerle et al. 2000; Isobe et al. 2003; Romanova et al. 2004).

The analysis of the ~30 largest flares in the COUP data by Favata et al. (2005) suggests that very long magnetic structures (up to a few times 10^{12} cm) are present in some of the most active stars in our sample. Such large structures (tens of times the size of the star) may indicate a magnetic link between these stars and their disks. However, we note that very large loop lengths were derived for only a few of these flares; for the majority of the analyzed flares much smaller loop lengths were found.

Furthermore, our results in the previous sections show that, in general, the X-ray luminosity is strongly linked to stellar parameters like bolometric luminosity and mass but does not strongly depend on the presence or absence of circumstellar disks as traced by near-infrared excess emission. It is reasonable to conclude that although X-ray emission from magnetic star-disk interactions may be seen during some of the most intense flares, the bulk of the observed X-ray emission from ONC TTSs probably originates from more compact structures with geometries resembling solar coronal fields.

9.1.3. *X-Ray Emission from Solar-like Coronal Structures?*

Our data are generally consistent with the assumption that the observed X-ray emission originates from, in principle solar-like, coronal structures. The X-ray luminosities and plasma temperatures derived for the ONC TTSs are comparable to those of the most active MS stars and can thus be understood by assuming that stellar coronae in general are composed of X-ray–emitting structures similar to those present in the solar corona (e.g., Drake et al. 2000; Peres et al. 2004). Although the high X-ray luminosities of active MS stars and TTSs cannot be reproduced by simply filling the available coronal volume with solar-like active regions, coronal structures with higher plasma density[20] can explain the high levels of stellar X-ray activity. Evidence for higher than solar plasma densities is found in high-resolution X-ray and EUV spectra for many active stars (e.g., Sanz-Forcada et al. 2003; Ness et al. 2004). Furthermore, once the stellar coronae get nearly completely filled with active regions, the magnetic interaction of the active regions should lead to increased flaring in the most active stars, boosting their X-ray luminosities even further (Peres et al. 2004).

We also note that the temporal behavior of most flares seen in the COUP data is rather similar to what is seen in flares on the Sun or active MS stars (Wolk et al. 2005). Further evidence suggesting enhanced solar-like coronal activity as the source of the X-ray emission from active MS stars and TTSs is summarized, for example, in Feigelson & Montmerle (1999) and Favata & Micela (2003).

9.2. *The Suppression of X-Ray Emission by Accretion*

Our COUP data confirm previous results that accreting TTSs show lower levels of X-ray activity than nonaccretors (Stelzer & Neuhäuser 2001; Flaccomio et al. 2003b; Stassun et al. 2004a). Here we discuss some possible explanations for this effect. Two previously suggested explanations can essentially be ruled out by our data. The first one is the suggestion that the systematically higher extinction of the accreting CTTSs (due to absorption in the accretion disk) may be responsible for their weaker *observed* X-ray emission as compared to the WTTSs (e.g., Stassun et al. 2004a). In our COUP data, individual extinction-corrected X-ray luminosities could be determined in a self-consistent fitting analysis of the individual X-ray spectra. The different levels of extinction in the accreting and nonaccreting stars should not lead to errors in the extinction-corrected X-ray luminosities.

We can also exclude the idea that accreting TTSs are weaker X-ray emitters because their rotation is braked by magnetic disk locking, leading to weaker dynamo action and therefore less X-ray emission than in the nonbraked WTTSs. We have shown in § 5.1 that neither the accretors nor the nonaccretors show a relation between rotation and X-ray activity, and thus the difference in rotation rates cannot be the reason for the difference in the level of X-ray emission.

9.2.1. *Accretion Changes the Magnetic Field Structure?*

Numerical simulations suggest that the pressure of the accreting material can distort the large-scale stellar magnetic field considerably (e.g., Miller & Stone 1997; Romanova et al. 2004) and the magnetospheric transfer of material to the star can give rise to instabilities of the magnetic fields around the inner disk edge and cause reconnection events. The presence of accreting material also leads to higher densities in (parts of) the magnetosphere. In contrast to the WTTSs, which probably have loops with moderate plasma densities, some fraction of the magnetic field lines in CTTSs would be mass loaded and therefore have much (~100 times) higher densities. If a magnetic reconnection event now liberates a certain amount of energy, this can heat the plasma in the low-density loops of WTTSs to X-ray–emitting temperatures ($\gtrsim$10 MK), while the denser plasma in the mass-loaded loops of the CTTSs would be heated to much lower temperatures and remain too cool to emit X-rays. This effect may cause the lower X-ray luminosities of the CTTSs as compared to WTTSs.

However, a more quantitative assessment of this model is difficult. According to magnetospheric accretion models, the fraction of the stellar surface that is covered by accretion funnels should be at most a few percent (e.g., Calvet & Gullbring 1998; Muzerolle et al. 2001). This may be too small a fraction to explain the reduction of the X-ray luminosity by a factor of ~2. On the other hand, we note that the estimates of the area of accretion funnels are uncertain, and other factors such as global changes in the topology of the magnetic field may play a (more?) important role. It therefore seems possible that magnetospheric accretion streams are somehow related to the different X-ray activity levels of accreting and nonaccreting stars. It is also interesting to note that the analysis of the largest flares in the COUP data by Favata et al. (2005) seems to indicate that intense, active accretion may inhibit magnetic heating of the accreting plasma, while in stars that are not actively accreting the long magnetic structures may acquire a "coronal" character.

9.2.2. *Accretion Changes the Stellar Structure?*

The accretion process may alter the internal stellar structure and the differential rotation patterns and thereby influence the magnetic field generation process. For example, Siess et al. (1999) found in their stellar evolution calculations that accretion reduces the efficiency of convection. This theoretical result agrees with another finding based on comparison of orbital masses of PMS stars with evolution models by Stassun et al. (2004b), who found that TTSs seem to have lower convection efficiencies than MS stars. The reduced convection efficiency may lead to weaker dynamo action.

Another effect may be that the magnetospheric star-disk coupling affects the differential rotation pattern at the stellar

[20] Remember that the emission measure, $\int n^2\, dV$, scales linearly with the plasma volume V, but with the square of the density n.

surface. If the coupling happens closer to the stellar equator than to the poles, the magnetospheric braking effect thought to be at work in CTTSs may reduce the amount of differential rotation, and this also may decrease the efficiency of the dynamo.

Finally, the magnetic star-disk interaction may also have an effect on the coupling between inner and outer layers within the star and thereby affect the level of magnetic activity (see Barnes 2003a, 2003b).

9.3. *Implications for PMS Magnetic Dynamos*

The MS activity-rotation relation is well established in stars (e.g., Pallavicini et al. 1981; Pizzolato et al. 2003) and is usually interpreted in terms of the α-Ω-type dynamo that is thought to work in the Sun. A simplified description of the rather complicated processes by which this dynamo generates surface magnetic fields can be summarized as follows (for details see, e.g., Schrijver & Zwaan 2000; Ossendrijver 2003): The strong differential rotation in the tachocline, a region near the bottom of the convection zone in which the rotation rate changes from being almost uniform in the radiative interior to being latitude dependent in the convection zone, generates strong toroidal magnetic fields. While most of the toroidal magnetic flux is stored and further amplified in the tachocline, instabilities expel individual flux tubes, which then rise through the convection zone, driven by magnetic buoyancy, until they emerge at the surface as active regions. The power of the dynamo (i.e., the magnetic energy created by the dynamo per unit time) depends only indirectly on the rotation rate. The α-Ω dynamo is principally dependent on the radial gradient of the angular velocity in the tachocline and the characteristic scale length of convection at the base of the convection zone. The empirical relationship between X-ray luminosity and rotation rate in MS stars does therefore *not* mean that the power of the dynamo scales with rotation rate, but rather that faster rotating stars have stronger velocity shear in the thin tachoclinal layer between the radiative core and the outer convective zone.

The presence of an α-Ω-type dynamo at the bottom of the convection zone does not prevent other dynamo processes from *also* operating in a star. In the Sun, small-scale turbulent dynamo action (e.g., Durney et al. 1993) is taking place throughout the convection zone and is thought to be responsible for the small-scale intranetwork fields. Recent results (Bueno et al. 2004) suggest that the total magnetic flux generated by the small-scale turbulent dynamo action is much larger than previously assumed. This means that two conceptually distinct magnetic dynamos are simultaneously operating in the contemporary Sun. In the case of the Sun, the coronal activity is most likely dominated by the tachoclinal dynamo action. Most of the ONC TTSs, however, are thought to be fully convective, or nearly fully convective, so the tachoclinal layer is either buried very deeply or does not exist at all. It is therefore reasonable to assume that in these (nearly) fully convective TTSs, a convective dynamo is the main source of the magnetic activity.

An interesting possible alternative explanation may be that the conventional wisdom, i.e., that TTSs are fully convective, is not correct. We note that several studies have shown that accretion can significantly change the stellar structure. For example, Prialnik & Livio (1985) found that even for moderate accretion rates the stars are no longer fully convective. More recently, Wuchterl & Tscharnuter (2003) found that accreting PMS stars are not fully convective; their model of a solar mass star at 1 Myr has a radiative core and a convective envelope, resembling the present Sun rather than a fully convective object. These results open the possibility for a solar-type tachoclinal dynamo to work in the TTSs. Our results on the relation between X-ray activity and Rossby number are not inconsistent with that possibility.

We provide in this study various empirical relationships of the X-ray luminosities with, e.g., stellar mass or bolometric luminosity, which should also be relevant to the dynamos operating in TTSs. A purely empirical explanation of these correlations is given by the existence of upper and lower limits to the X-ray activity levels, in analogy to results for MS stars. The upper limit is caused by the saturation level of magnetic activity around $\log(L_{\rm X}/L_{\rm bol}) \sim -3$ (e.g., Pizzolato et al. 2003). A lower limit is suggested by studies of nearby field stars, which led to the conclusion that all cool dwarf stars are surrounded by X-ray–emitting coronae with a minimum X-ray surface flux of about 1×10^4 ergs cm^{-2} s^{-1} (Schmitt 1997; Schmitt & Liefke 2004); for early M-type TTSs in the ONC this surface flux corresponds to $\log(L_{\rm X}/L_{\rm bol}) \sim -6$. The restriction of $\log(L_{\rm X}/L_{\rm bol})$ to the range between about -6 and -3 leads to correlation between X-ray luminosity and bolometric luminosity; the correlation between X-ray luminosity and stellar mass can then be explained by the dependence of bolometric luminosity on stellar mass. An alternative explanation for the correlations can be based on the finding that the fractional X-ray luminosities increase with stellar mass (§ 4.2). This is consistent with the results of Pizzolato et al. (2003), who showed that in low-mass MS stars the saturation level in $L_{\rm X}/L_{\rm bol}$ increases with stellar mass. These results suggest a similar origin of X-ray activity in the TTSs and MS stars, and thus provide support for the standard α-Ω solar-type dynamo model for TTS X-ray emission.

10. SUMMARY

The main results from our study of the X-ray properties of the TTSs in the ONC can be summarized as follows. In the COUP data we detect X-ray emission from essentially every late-type (F–M) ONC star. There is no indication for the existence of an "X-ray–quiet" population of stars with suppressed magnetic activity. We find that the X-ray luminosities of the TTSs are correlated to bolometric luminosities, stellar masses, and effective temperatures. The $L_{\rm X} \leftrightarrow M$ correlation for the TTSs shows a slope similar to the corresponding correlation for MS stars, which is probably related to the association between mass and MS X-ray saturation levels. Together, these lines of evidence suggest that the $L_{\rm X} \leftrightarrow M$ relationship may be more physically fundamental than X-ray relationships to bolometric luminosity, surface area, or rotation.

Our data indicate a correlation between X-ray activity and rotation period, apparently in strong contrast to the well-established anticorrelation seen for MS stars. However, the efficacy of our analysis is limited, since rotation periods are only known for about 40% of the TTSs in our sample and the missing stars (i.e., those with unknown rotation periods) probably introduce a bias. If we consider Rossby numbers, we find that all TTSs are located in the saturated or supersaturated regime of the activity↔Rossby number relation for MS stars. In principle, the TTSs may thus follow the same relation between X-ray activity and Rossby number as do MS stars, but the large scatter in $L_{\rm X}/L_{\rm bol}$ at any given Rossby number suggests that other factors are also involved in determining the level of X-ray activity.

The enormous scatter we generally find in the correlations between X-ray activity and other stellar parameters is larger than what one would expect due to X-ray variability, uncertainties in the variables, and the effects of unresolved binaries. Therefore, this wide scatter must be related to intrinsic differences in the individual TTSs, and we find here that the influence of accretion on the X-ray emission seems to play an important role. There is a

remarkable contrast between the X-ray properties of accreting and nonaccreting stars: Our data confirm previous results that accreting stars are less X-ray active than nonaccreting stars (although a statistically significant difference is only found for stars in the $\sim$0.2–0.5 $M_{\odot}$ mass range) and suggest an anticorrelation between fractional X-ray luminosity and accretion rate. The nonaccreting TTSs have the same median X-ray activity level as rapidly rotating MS stars and show good $L_X \leftrightarrow L_{bol}$ and $L_X \leftrightarrow M$ correlations with a scatter as expected from the uncertainties, X-ray variability, and unresolved binaries. The accreting TTSs, on the other hand, show X-ray activity levels about 3 times lower and produce much less well-defined $L_X \leftrightarrow L_{bol}$ and $L_X \leftrightarrow M$ correlations with much wider scatter. These findings imply that the apparent X-ray deficit of the whole TTS sample [i.e., the median fractional X-ray luminosity of $\log(L_X/L_{bol}) \sim -3.5$, which is below the saturation limit around $\log(L_X/L_{bol}) \sim -3.0$ typically found for rapidly rotating MS stars] is solely due to the reduced X-ray activity of the accreting TTSs.

We discuss several possible explanations for the suppression of X-ray emission in accreting stars. The effect may be related to changes of the coronal structure or the internal stellar structure induced by the accretion process. We favor the idea that magnetic reconnection cannot heat the dense plasma in mass-loaded accreting field lines to X-ray temperatures.

The geometry of X-ray–producing magnetic fields is also still uncertain. Solar-type coronal loops are probably the dominant source of the observed X-ray emission. However, we note that the study of the most powerful flares seen in COUP stars (Favata et al. 2005) suggests that in some objects star-disk field lines extending $>10R_*$ from the stellar surface may be involved. Accretion shocks at the stellar surface cannot be responsible for the emission seen in COUP sources. Finally, the ultimate origin of the X-ray activity of the TTSs is most likely either a turbulent dynamo working in the stellar convection zone, or, if theoretical suggestions that accreting TTSs may not be fully convective are correct, a solar-like α-Ω dynamo at the base of the convection zone.

COUP is supported by *Chandra* Guest Observer grant SAO GO3-4009A (PI: E. Feigelson). Further support was provided by the *Chandra* ACIS Team contract NAS8-38252. We would like to thank Lynne A. Hillenbrand for useful comments on the manuscript. We are grateful to Juergen Schmitt and Carolin Liefke for their generous sharing of NEXXUS results, Hardi Peter for enlightening discussion about the solar corona, Matthias Hünsch for information about the X-ray luminosities of subgiants, and Hsien Shang for discussions about accretion processes. Y. C. K. has been supported by Korean Research Foundation Grant KRF-2002-070-C00045. B. S., E. F., G. M., and S. S. acknowledge financial support from an Italian MIUR PRIN program and an INAF program for the years 2002–2004.

Facilities: CXO (ACIS)

REFERENCES

Alcalá, J. M., et al. 1996, A&AS, 199, 7
Alexander, D. R., & Ferguson, J. W. 1994, ApJ, 437, 879
Aschwanden, M. J., Poland, A. I., & Rabin, D. M. 2001, ARA&A, 39, 175
Bahcall, J. N., & Pinsonneault, M. H. 1992, Rev. Mod. Phys., 60, 297
Bahcall, J. N., Serenelli, A. M., & Pinsonneault, M. H. 2004, ApJ, 614, 464
Barnes, S. A. 2003a, ApJ, 586, 464
———. 2003b, ApJ, 586, L145
Brickhouse, N. S., et al. 2000, ApJ, 530, 387
Briggs, K. R., & Pye, J. P. 2003, MNRAS, 345, 714
Bueno, J. T., Shchukina, N., & Ramos, A. A. 2004, Nature, 430, 326
Calvet, N., & Gullbring, E. 1998, ApJ, 509, 802
Casanova, S., Montmerle, T., Feigelson, E. D., & André, P. 1995, ApJ, 439, 752
Drake, J. 2005, in Proc. 13th Cool Stars and Stellar Systems Workshop, ed. F. Favata & G. Hussain (ESA-SP 560; Noordwijk: ESA), 519
Drake, J. J., Peres, G., Orlando, S., Laming, J., & Maggio, A. 2000, ApJ, 545, 1074
Durney, B. R., De Young, D. S., & Roxburgh, I. W. 1993, Sol. Phys., 145, 207
Favata, F., Giardino, G., Micela, G., Sciortino, S., & Damiani, F. 2003, A&A, 403, 187
Favata, F., & Micela, G. 2003, Space Sci. Rev., 108, 577
Favata, F., et al. 2004, A&A, 418, L13
———. 2005, ApJS, 160, 469
Feigelson, E. D., & Babu, G. J. 1992, ApJ, 397, 55
Feigelson, E. D., Broos, P., Gaffney, J. A., Garmire, G., Hillenbrand, L. A., Pravdo, S. H., Townsley, L., & Tsuboi, Y. 2002a, ApJ, 574, 258
Feigelson, E. D., Casanova, S., Montmerle, T., & Guibert, J. 1993, ApJ, 416, 623
Feigelson, E. D., & DeCampli, W. M. 1981, ApJ, 243, L89
Feigelson, E. D., Gaffney, J. A., Garmire, G., Hillenbrand, L. A., & Townsley, L. 2003, ApJ, 584, 911
Feigelson, E. D., Garmire, G. P., & Pravdo, S. H. 2002b, ApJ, 572, 335
Feigelson, E. D., & Montmerle, T. 1999, ARA&A, 37, 363
Feigelson, E. D., & Nelson, P. I. 1985, ApJ, 293, 192
Flaccomio, E., Damiani, F., Micela, G., Sciortino, S., Harnden, F. R., Murray, S. S., & Wolk, S. J. 2003a, ApJ, 582, 382
———. 2003b, ApJ, 582, 398
Flaccomio, E., et al. 2005, ApJS, 160, 450
Fleming, T. A., Liebert, J., Giao, I. M., & Maccacaro, M. 1988, ApJ, 331, 958
Fleming, T. A., Schmitt, J. H. M. M., & Giampapa, M. S. 1995, ApJ, 450, 401
Gagné, M., Caillault, J.-P., & Stauffer, J. R. 1995, ApJ, 445, 280
Garmire, G., Feigelson, E. D., Broos, P., Hillenbrand, L. A., Pravdo, S. H., Townsley, L., & Tsuboi, Y. 2000, AJ, 120, 1426
Geier, S., Wendker, H. J., & Wisotzki, L. 1995, A&A, 229, 39
Getman, K. V., et al. 2005a, ApJS, 160, 319
Giampapa, M. S., Rosner, R., Kashyap, V., Fleming, T. A., Schmitt, J. H. M. M., & Bookbinder, J. A. 1996, ApJ, 463, 707
Gilliland, R. L. 1986, ApJ, 300, 339
Glassgold, A. E., Feigelson, E. D., & Montmerle, T. 2000, in Protostars and Planets IV, ed. V. Mannings, A. P. Boss, & S. S. Russell (Tucson: Univ. Arizona Press), 429
Grevesse, N., & Noels, A. 1993, in Origin and Evolution of the Elements, ed. N. Prantzos, E. Vangioni-Flam, & M. Casse (Cambridge: Cambridge Univ. Press), 14
Grevesse, N., Noels, A., & Sauval, A. J. 1996, in ASP Conf. Ser. 99, Cosmic Abundances, ed. S. S. Holt & G. Sonneborn (San Francisco: ASP), 117
Grosso, N., et al. 2005, ApJS, 160, 530
Güdel, M., Guinan, E. F., & Skinner, S. L. 1997, ApJ, 483, 947
Gullbring, E., Barwig, H., & Schmitt, J. H. M. M. 1997, A&A, 324, 155
Haisch, K. E., Lada, E. A., Pina, R. K., Telesco, C. M., & Lada, C. J. 2001, AJ, 121, 1512
Hayashi, M. R., Shibata, K., & Matsumoto, R. 1996, ApJ, 468, L37
Herbig, G. H., & Terndrup, D. M. 1986, ApJ, 307, 609
Hillenbrand, L. A. 1997, AJ, 113, 1733 (H97)
Hillenbrand, L. A., Strom, S. E., Calvet, N., Merrill, K. M., Gatley, I., Makidon, R. B., Meyer, M. R., & Skrutskie, M. F. 1998, AJ, 116, 1816
Hillenbrand, L. A., & White, R. J. 2004, ApJ, 604, 741
Iglesias, C. A., & Rogers, F. J. 1996, ApJ, 464, 943
Isobe, H., Shibata, K., Yokoyama, T., & Imanishi, K. 2003, PASJ, 55, 967
Isobe, T., Feigelson, E. D., Akritas, M. G., & Babu, G. J. 1990, ApJ, 364, 104
Isobe, T., Feigelson, E. D., & Nelson, P. I. 1986, ApJ, 306, 490
Itoh, N., Adachi, T., Nagakawa, M., Kohyama, Y., & Munakata, H. 1989, ApJ, 339, 354 (erratum 360, 741)
Judge, P. G., Solomon, S. C., & Ayres, T. R. 2003, ApJ, 593, 534
Kastner, J. H., Huenemoerder, D. P., Schulz, N. S., Canizares, C. R., & Weintraub, D. A. 2002, ApJ, 567, 434
Kim, Y.-C., & Demarque, P. 1996, ApJ, 457, 340
Kim, Y.-C., Fox, P. A., Demarque, P., & Sofia, S. 1996, ApJ, 461, 499
Ku, W. H.-M., & Chanan, G. A. 1979, ApJ, 234, L59
Küker, M., & Rüdiger, G. 1999, A&A, 346, 922
Lamzin, S. A., et al. 1996, A&A, 306, 877
La Valley, M., Isobe, T., & Feigelson, E. D. 1990, BAAS, 22, 917
Luhman, K. L. 1999, ApJ, 525, 466
Maggio, A., et al. 1987, ApJ, 315, 687
Matsumura, S., & Pudritz, R. E. 2003, ApJ, 598, 645

McCaughrean, M. J., & Stauffer, J. R. 1994, AJ, 108, 1382
Messina, S., Pizzolato, N., Guinan, E. F., & Rodono, M. 2003, A&A, 410, 671
Micela, G., & Marino, A. 2003, A&A, 404, 637
Miller, K. A., & Stone, J. M. 1997, ApJ, 489, 890
Montesinos, B., Thomas, J. H., Ventura, P., & Mazzitelli, I. 2001, MNRAS, 326, 877
Montmerle, T., Grosso, N., Tsuboi, Y., & Koyama, K. 2000, ApJ, 352, 1097
Muzerolle, J., Calvet, N., & Hartmann, L. 2001, ApJ, 550, 944
Ness, J.-U., Güdel, M., Schmitt, J. H. M. M., Audard, M., & Telleschi, A. 2004, A&A, 427, 667
Neuhäuser, R. 1997, Science, 276, 1363
Neuhäuser, R., Sterzik, M. F., Schmitt, J. H. M. M., Wichmann, R., & Krautter, J. 1995, A&A, 297, 391
O'Dell, C. R. 2001, ARA&A, 39, 99
Orlando, S., Peres, G., & Reale, F. 2004, A&A, 424, 677
Ossendrijver, M. 2003, A&A Rev., 11, 287
Palla, F., & Stahler, S. W. 1993, ApJ, 418, 414
———. 1999, ApJ, 525, 772 (PS)
Pallavicini, R., Golub, L., Rosner, R., Vaiana, G. S., Ayres, T., & Linsky, J. L. 1981, ApJ, 248, 279
Peres, G., Orlando, S., & Reale, F. 2004, ApJ, 612, 472
Pillitteri, I., Micela, G., Sciortino, S., Damiani, F., & Harnden, F. R., Jr. 2004, A&A, 421, 175
Pizzolato, N., Maggio, A., Micela, G., Sciortino, S., & Ventura, P. 2003, A&A, 397, 147
Preibisch, Th. 1997, A&A, 320, 525
Preibisch, Th., & Feigelson, E. D. 2005, ApJS, 160, 390
Preibisch, Th., & Zinnecker, H. 2002, AJ, 123, 1613
Preibisch, Th., Zinnecker, H., & Herbig, G. H. 1996, A&A, 310, 456
Preibisch, Th., et al. 2005, ApJS, 160, 582
Prialnik, D., & Livio, M. 1985, MNRAS, 216, 37
Robberto, M., Song, J., Mora Carrillo, G., Beckwith, S. V. W., Makidon, R. B., & Panagia, N. 2004, ApJ, 606, 952
Rogers, F. J., Swenson, F. J., & Iglesias, C. A. 1996, ApJ, 456, 902
Romanova, M. M., Ustyugova, G. V., Koldoba, A. V., & Lovelace, R. V. E. 2004, ApJ, 616, L151
Sanz-Forcada, J., Brickhouse, N. S., & Dupree, A. K. 2003, ApJS, 145, 147
Schmitt, J. H. M. M. 1997, A&A, 318, 215
Schmitt, J. H. M. M., & Liefke, C. 2004, A&A, 417, 651
Schmitt, J. H. M. M., Robrade, J., Ness, J.-U., Favata, F., & Stelzer, B. 2005, A&A, 432, L35
Schrijver, C. J., & Zwaan, C. 2000, Solar and Stellar Magnetic Activity (New York: Cambridge Univ. Press)
Schulz, N. S., Canizares, C., Huenemoerder, D., Kastner, J. H., Taylor, S. C., & Bergstrom, E. J. 2001, ApJ, 549, 441
Schulz, N. S., Canizares, C. R., Huenemoerder, D., & Lee, J. C. 2000, ApJ, 545, L135
Schulz, N. S., Canizares, C., Huenemoerder, D., & Tibbets, K. 2003, ApJ, 595, 365
Siess, L., Dufour, E., & Forestini, M. 2000, A&A, 358, 593 (SDF)
Siess, L., Forestini, M., & Bertout, C. 1999, A&A, 342, 480
Skinner, S., Gagné, M., & Belzer, E. 2003, ApJ, 598, 375
Stassun, K. G., Ardila, D. R., Barsony, M., Basri, G., & Mathieu, R. D. 2004a, AJ, 127, 3537
Stassun, K. G., Mathieu, R. D., Vaz, L. P. R., Stroud, N., & Vrba, F. J. 2004b, ApJS, 151, 357
Stassun, K. G., et al. 2005, ApJ, submitted
Stelzer, B., & Neuhäuser, R. 2001, A&A, 377, 538
Stelzer, B., & Schmitt, J. H. M. M. 2004, A&A, 418, 687
Stelzer, B., et al. 2005, ApJS, 160, 557
Thoul, A. A., Bahcall, J. N., & Loeb, A. 1994, ApJ, 421, 828
Walsh, R. W., & Ireland, J. 2003, A&A Rev., 12, 1
Walter, F. M., Brown, A., Mathieu, R. D., & Myers, P. C. 1988, AJ, 96, 297
Wolk, S., et al. 2005, ApJS, 160, 423
Wuchterl, G., & Tscharnuter, W. M. 2003, A&A, 398, 1081
Yamauchi, S., Koyama, K., Sakano, M., & Okada, K. 1996, PASJ, 48, 719
Yi, S., Demarque, P., Kim, Y.-C., Lee, Y. W., Ree, C. H., Lejeune, T., & Barnes, S. 2001, ApJS, 136, 417